

Hi!

Impact of LHC dark matter searches on new physics scenarios

Suchita Kulkarni
HEPHY, Vienna

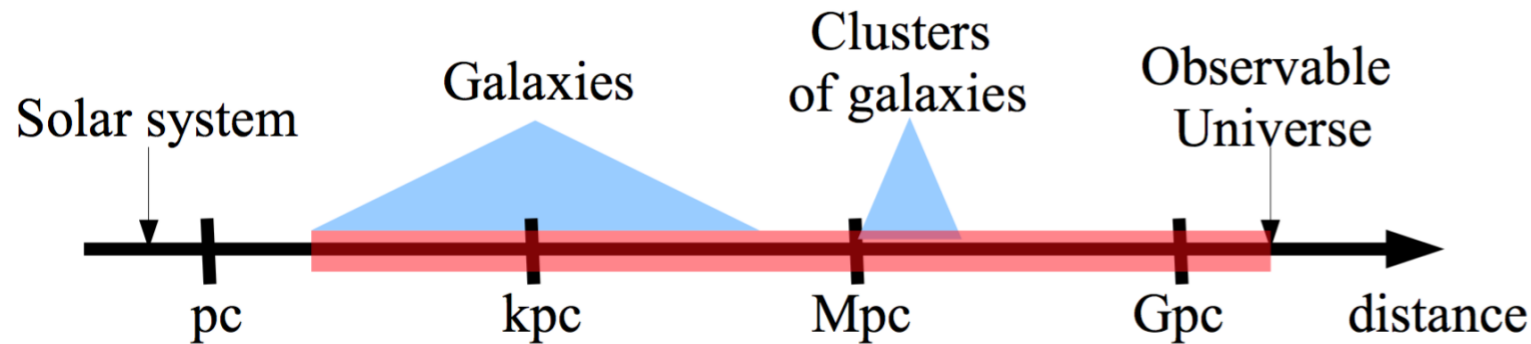
Based on:

arXiv:1512.06842 (D. Barducci, A. Goudelis, D. Sengupta) [Published JHEP]

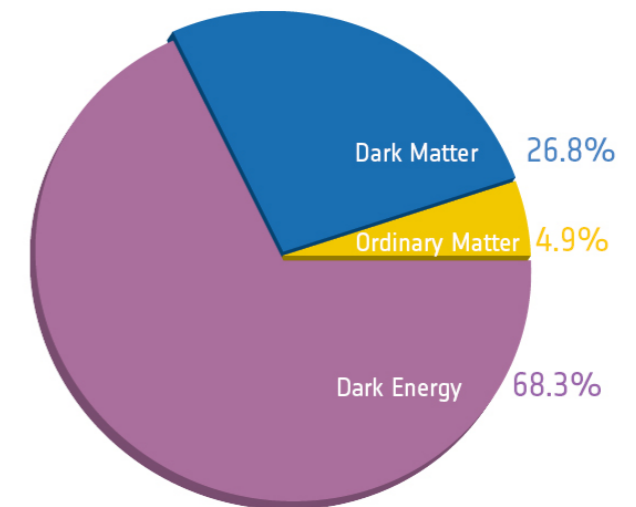
arXiv:1605.02684 (D. Barducci, A. Bharucha, N. Desai, M. Frigerio, B. Fuks, A. Goudelis, S. Lacroix, G. Polesello, D. Sengupta) [work in progress]

Dark matter

- Strong evidence on all scales



- Precise measurements of relic density



After Planck

- But apart from that...

DARK MATTER

$$J = ?$$

Mass $m = ?$
Mean life $\tau = ?$

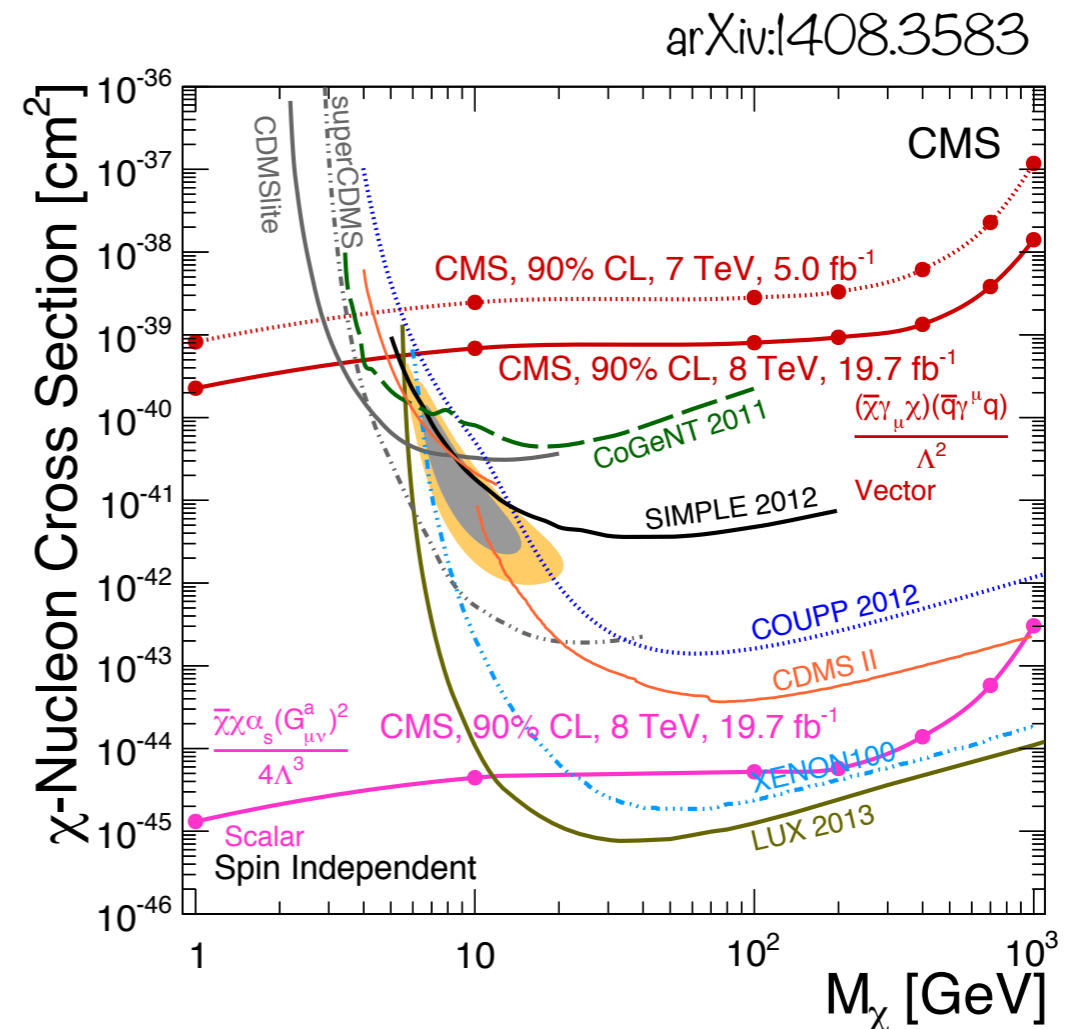
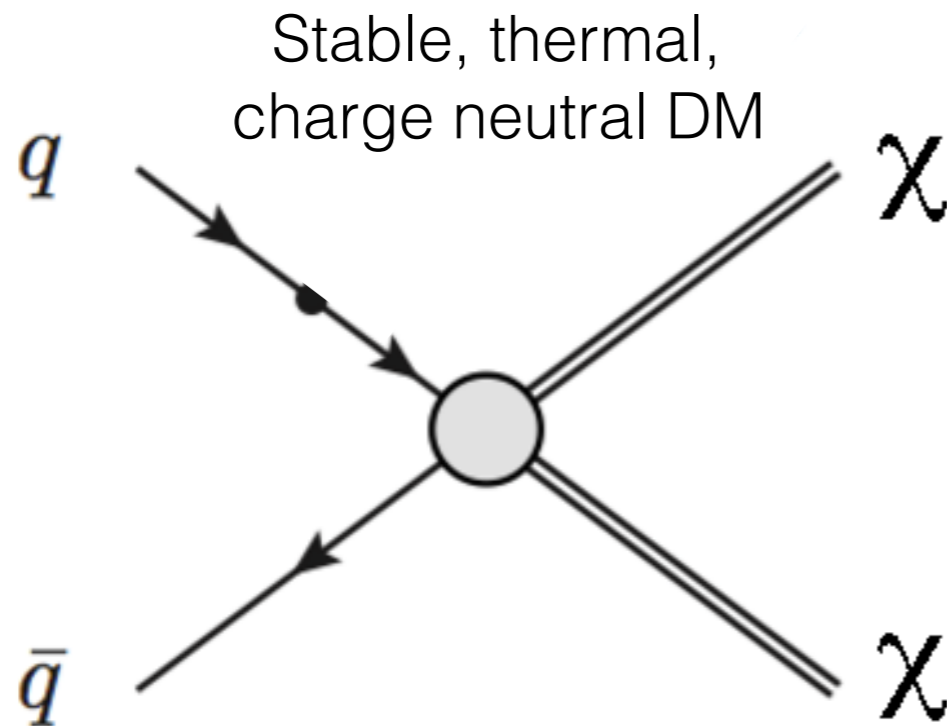
DECAY MODES	Fraction (Γ_i/Γ)	Confidence level	p (MeV/c)
?	?	?	?

Goal for 21st century:
identify the properties of
dark matter

• Talk by J. Schieck

- This talk: If dark matter is related to TeV scale physics, what can LHC tell us?

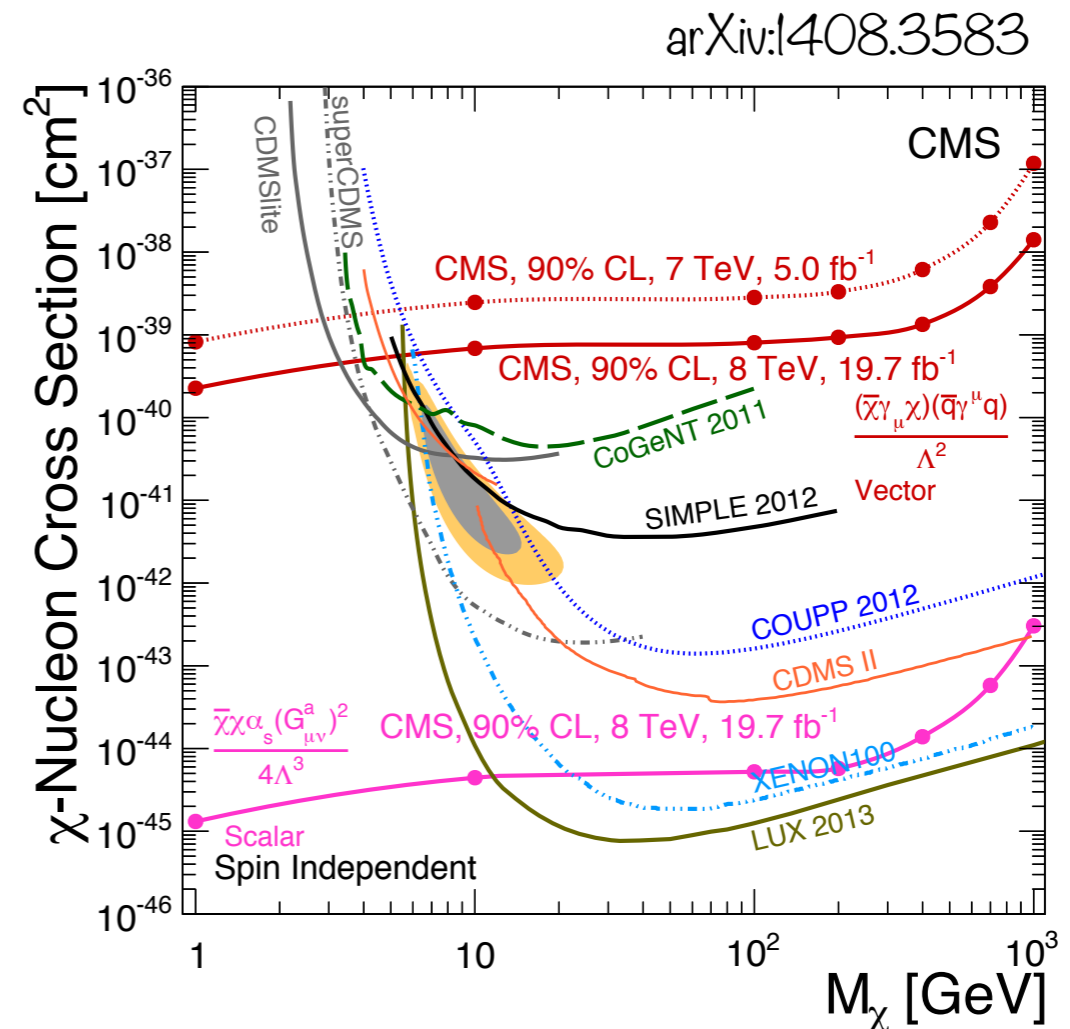
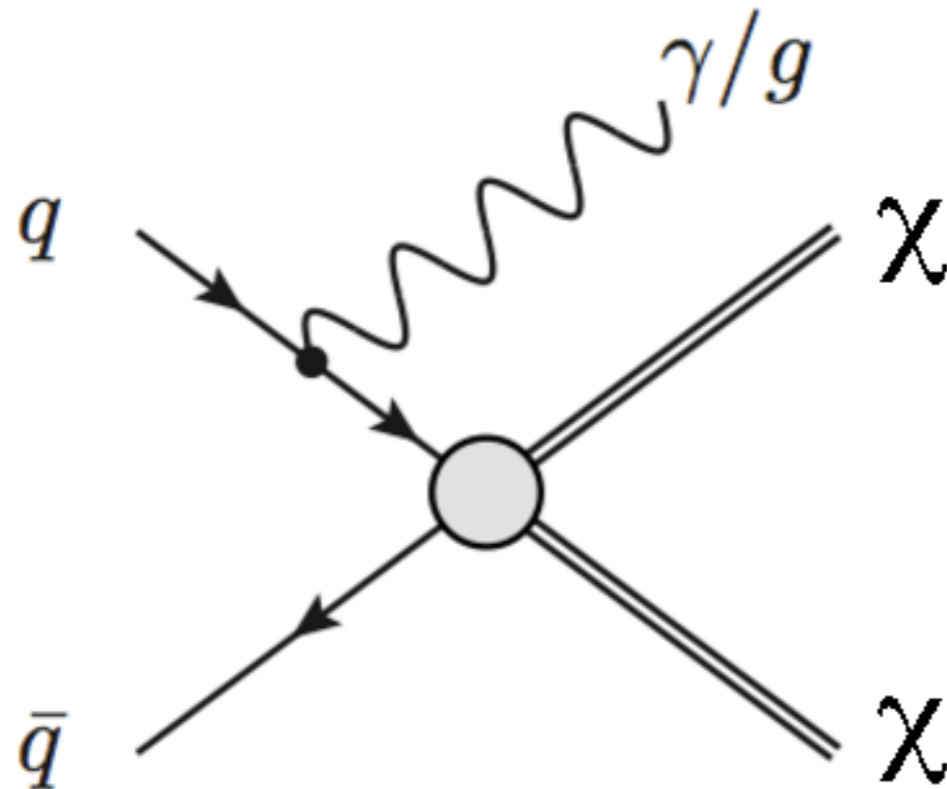
Hunt at the LHC



- Derived limits often depend on exact theoretical scenario, e.g. couplings, masses
- Necessary to reinterpret mono jet limits within a given theoretical scenario (extensive use of additional information given by LHC collaborations)
- This talk: usage of monojet searches to constrain two new physics scenarios

• NB: Effective operator description at the LHC is a dangerous way to set limits, interpret plots carefully

Hunt at the LHC

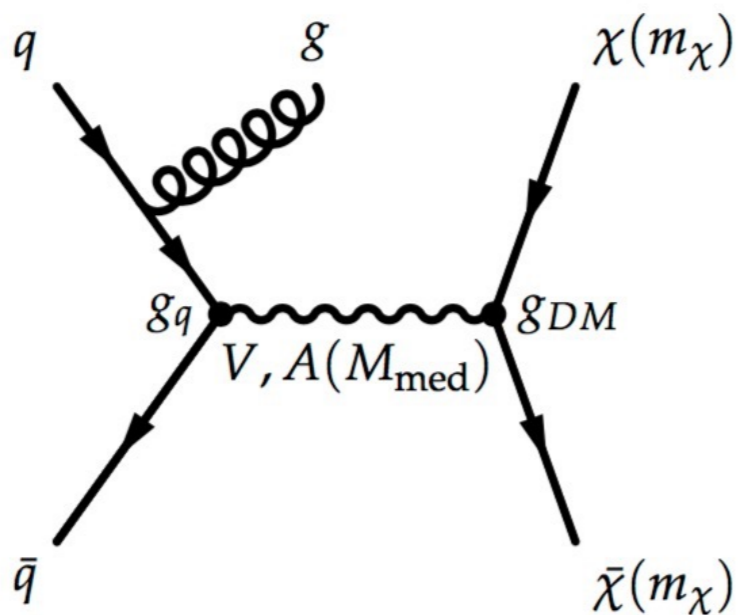


- Derived limits often depend on exact theoretical scenario, e.g. couplings, masses
- Necessary to reinterpret mono jet limits within a given theoretical scenario (extensive use of additional information given by LHC collaborations)
- This talk: usage of monojet searches to constrain two new physics scenarios

• NB: Effective operator description at the LHC is a dangerous way to set limits, interpret plots carefully

Hunt at the LHC

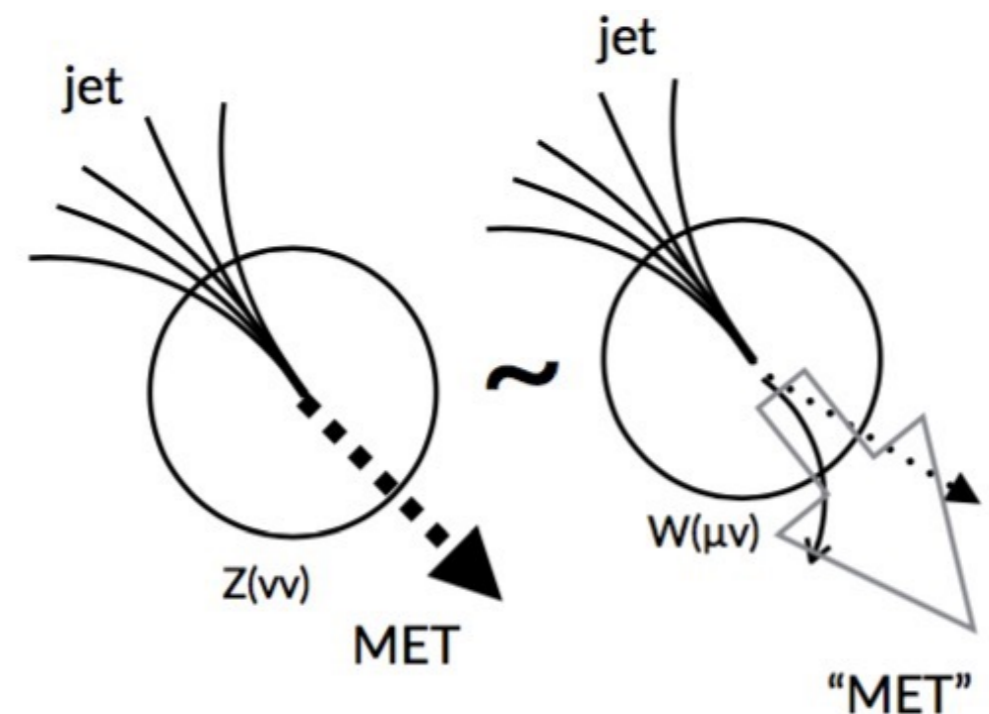
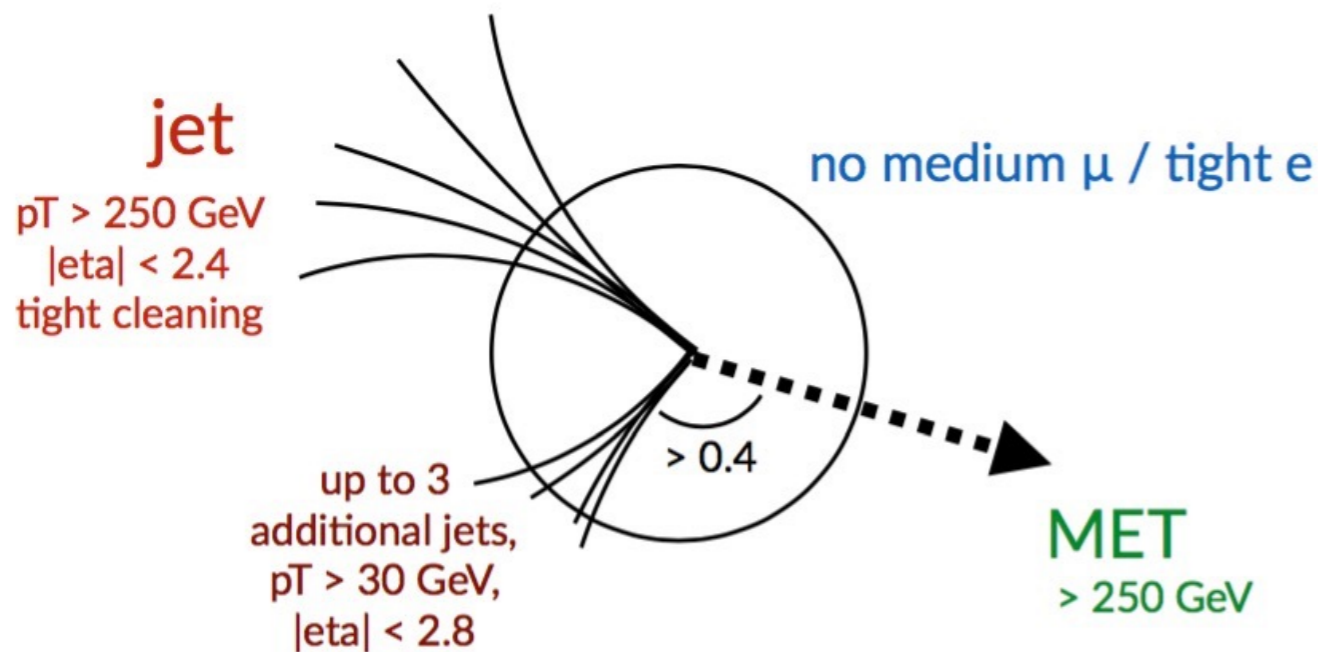
Figures courtesy A. Boveia's talk



- Signal regions with successively larger MET requirement

CMS-EXO-12-048

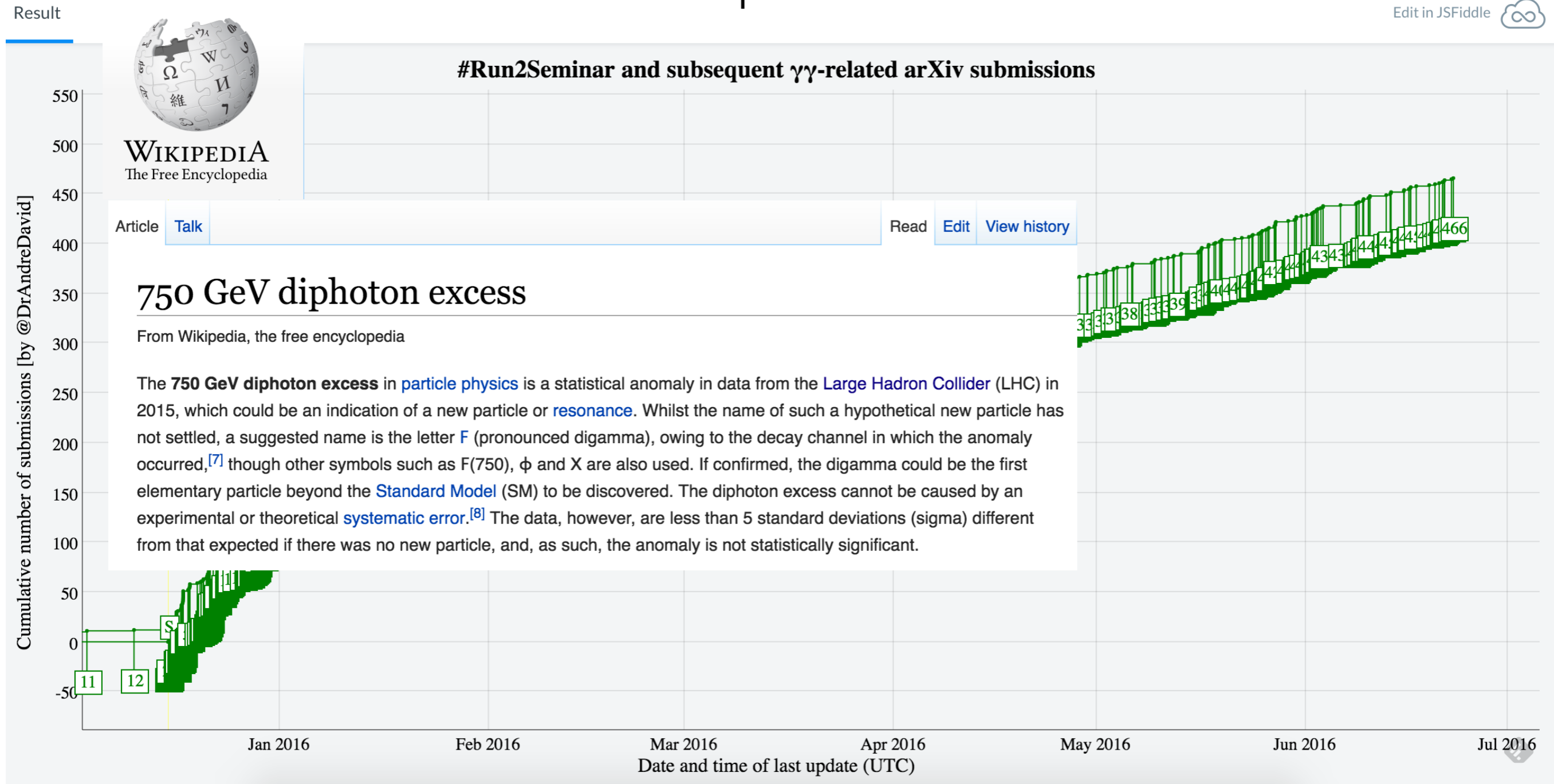
- MET > 250 GeV
- MET > 300 GeV
- MET > 350 GeV
- MET > 400 GeV
- MET > 450 GeV
- MET > 500 GeV
- MET > 550 GeV



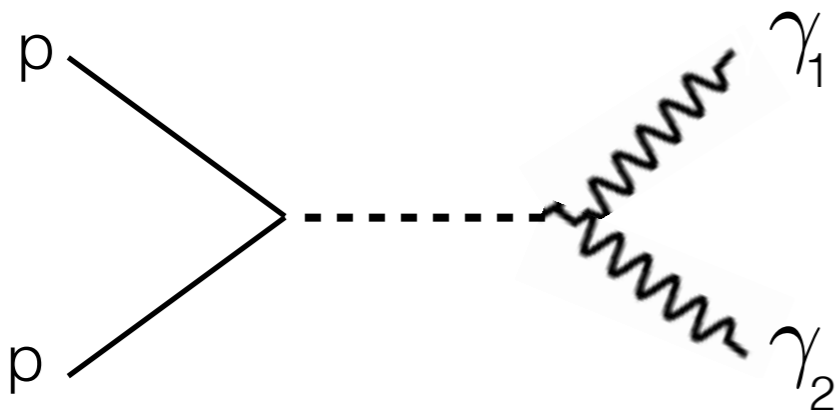
Test case: I

750 GeV as a portal to dark matter

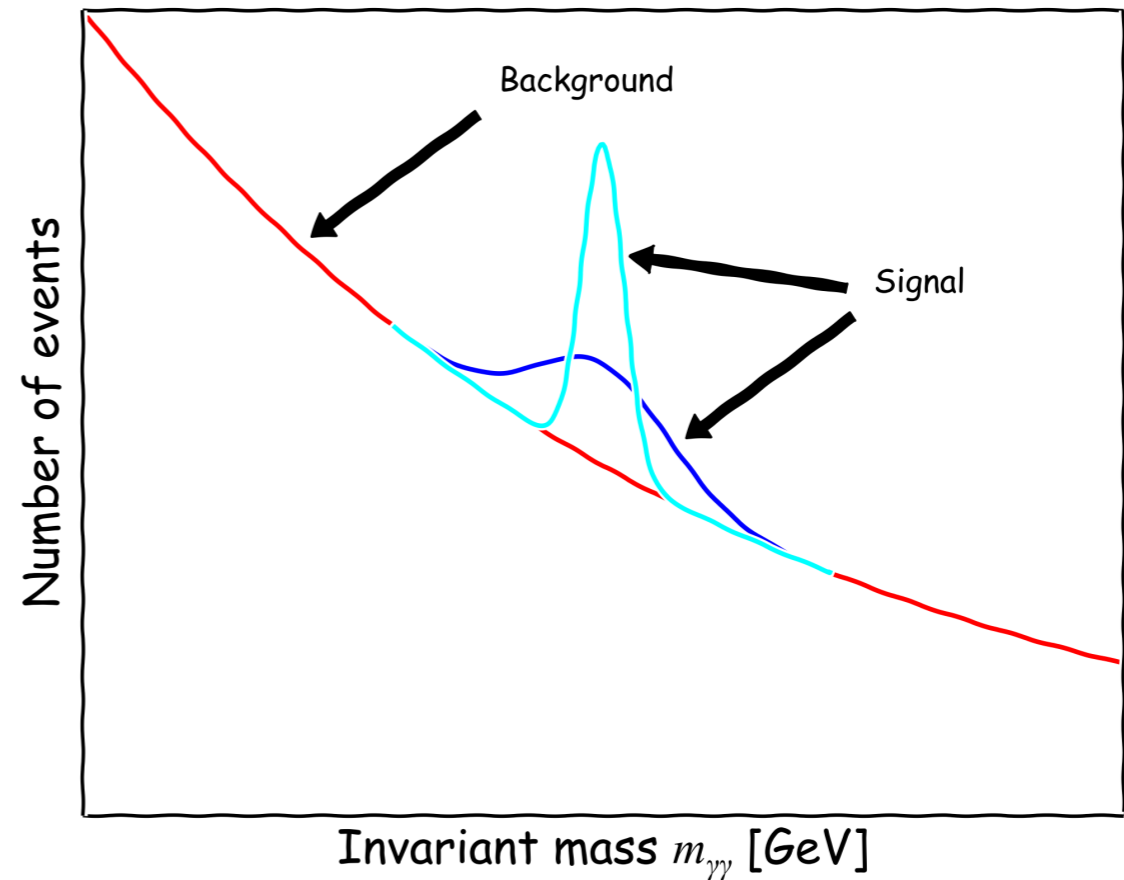
Edit in JSFiddle 



The 750 GeV buzz (fuss)

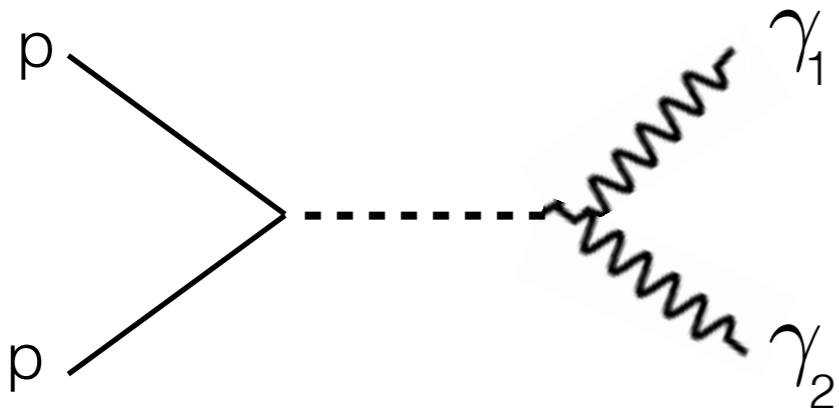


$$m_{\gamma\gamma}^2 = 2E_{\gamma_1}E_{\gamma_2}(1 - \cos\theta_{\gamma_1\gamma_2})$$

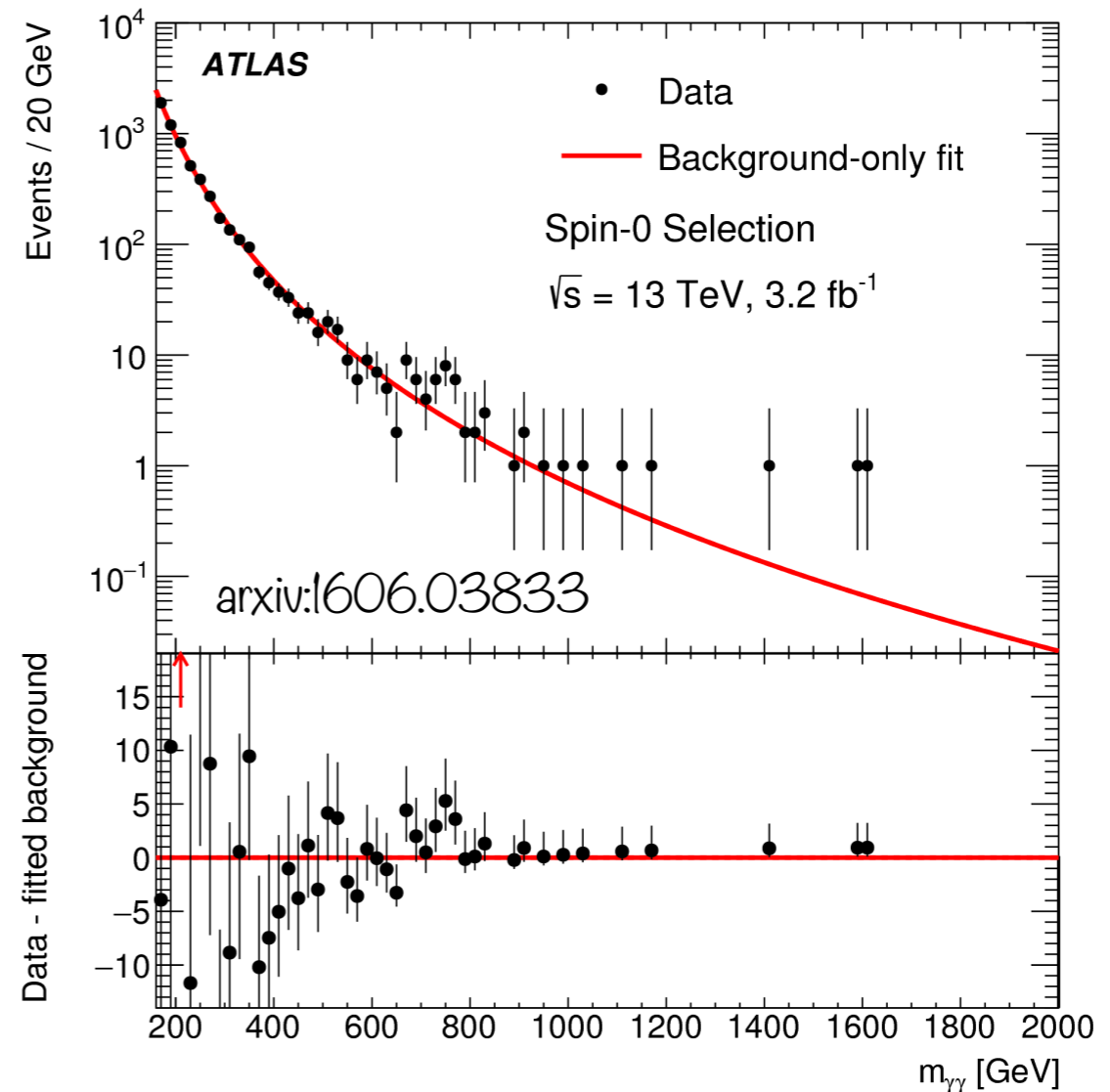


- ATLAS: 3.9σ local and 2.1σ global significance (13 TeV)
- CMS: 3.4σ local and 1.4σ global significance (8 + 13 TeV)
- Excess with large cross sections \sim few fb
- Not possible to obtain large width, cross section with couplings only to SM particles \rightarrow additional decay modes necessary

The 750 GeV buzz (fuss)



$$m_{\gamma\gamma}^2 = 2E_{\gamma_1}E_{\gamma_2}(1 - \cos\theta_{\gamma_1\gamma_2})$$



- ATLAS: 3.9σ local and 2.1σ global significance (13 TeV)
- CMS: 3.4σ local and 1.4σ global significance (8 + 13 TeV)
- Excess with large cross sections \sim few fb
- Not possible to obtain large width, cross section with couplings only to SM particles \rightarrow additional decay modes necessary

750 GeV portal to DM

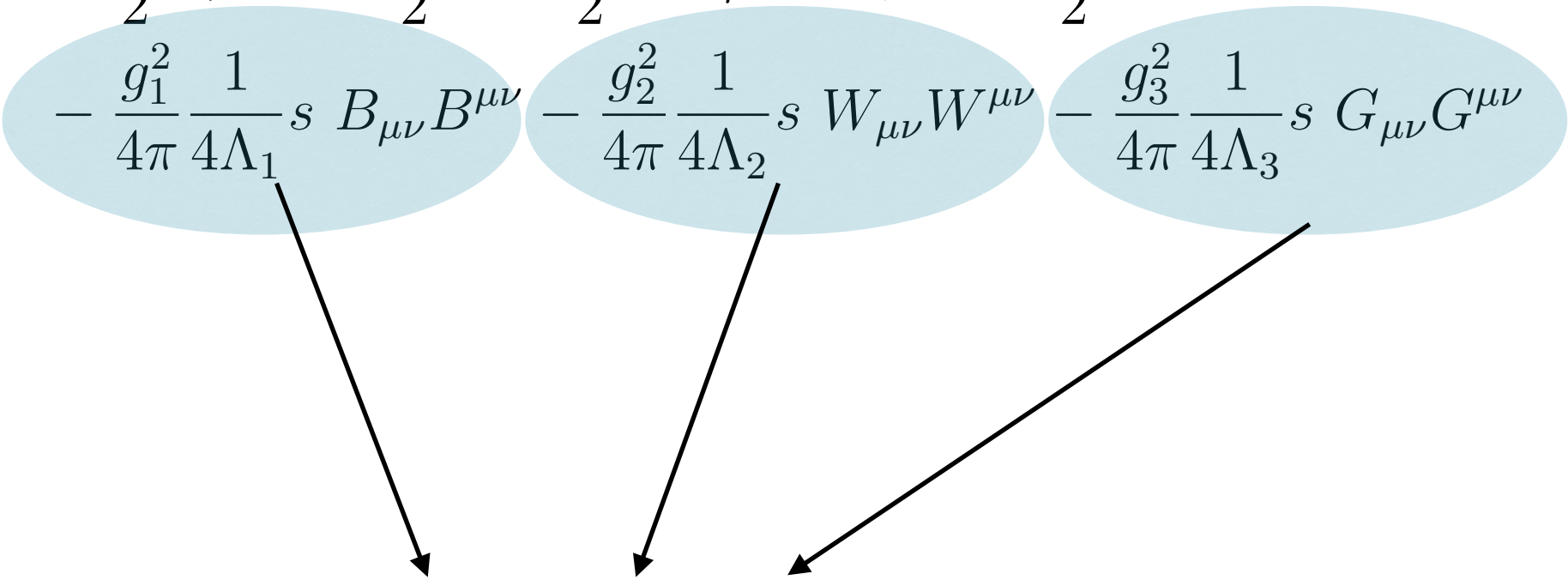
- Coupling of a 750 scalar resonance to gauge bosons and dark matter particle
- $d = 5$ effective Lagrangian, Majorana fermion dark matter

$$\begin{aligned} \mathcal{L}_{\text{NP,CPE}} = & \frac{1}{2}(\partial_\mu s)^2 - \frac{\mu_s^2}{2}s^2 + \frac{1}{2}\bar{\psi}(i\cancel{\partial}_\mu - m_\psi)\psi - \frac{y_\psi}{2}s\bar{\psi}\psi \\ & - \frac{g_1^2}{4\pi} \frac{1}{4\Lambda_1} s B_{\mu\nu}B^{\mu\nu} - \frac{g_2^2}{4\pi} \frac{1}{4\Lambda_2} s W_{\mu\nu}W^{\mu\nu} - \frac{g_3^2}{4\pi} \frac{1}{4\Lambda_3} s G_{\mu\nu}G^{\mu\nu} \end{aligned}$$

750 GeV portal to DM

- Coupling of a 750 scalar resonance to gauge bosons and dark matter particle
- $d = 5$ effective Lagrangian, Majorana fermion dark matter

$$\mathcal{L}_{\text{NP,CPE}} = \frac{1}{2}(\partial_\mu s)^2 - \frac{\mu_s^2}{2}s^2 + \frac{1}{2}\bar{\psi}(i\cancel{\partial}_\mu - m_\psi)\psi - \frac{y_\psi}{2}s\bar{\psi}\psi$$

$$- \frac{g_1^2}{4\pi} \frac{1}{4\Lambda_1} s B_{\mu\nu} B^{\mu\nu} - \frac{g_2^2}{4\pi} \frac{1}{4\Lambda_2} s W_{\mu\nu} W^{\mu\nu} - \frac{g_3^2}{4\pi} \frac{1}{4\Lambda_3} s G_{\mu\nu} G^{\mu\nu}$$


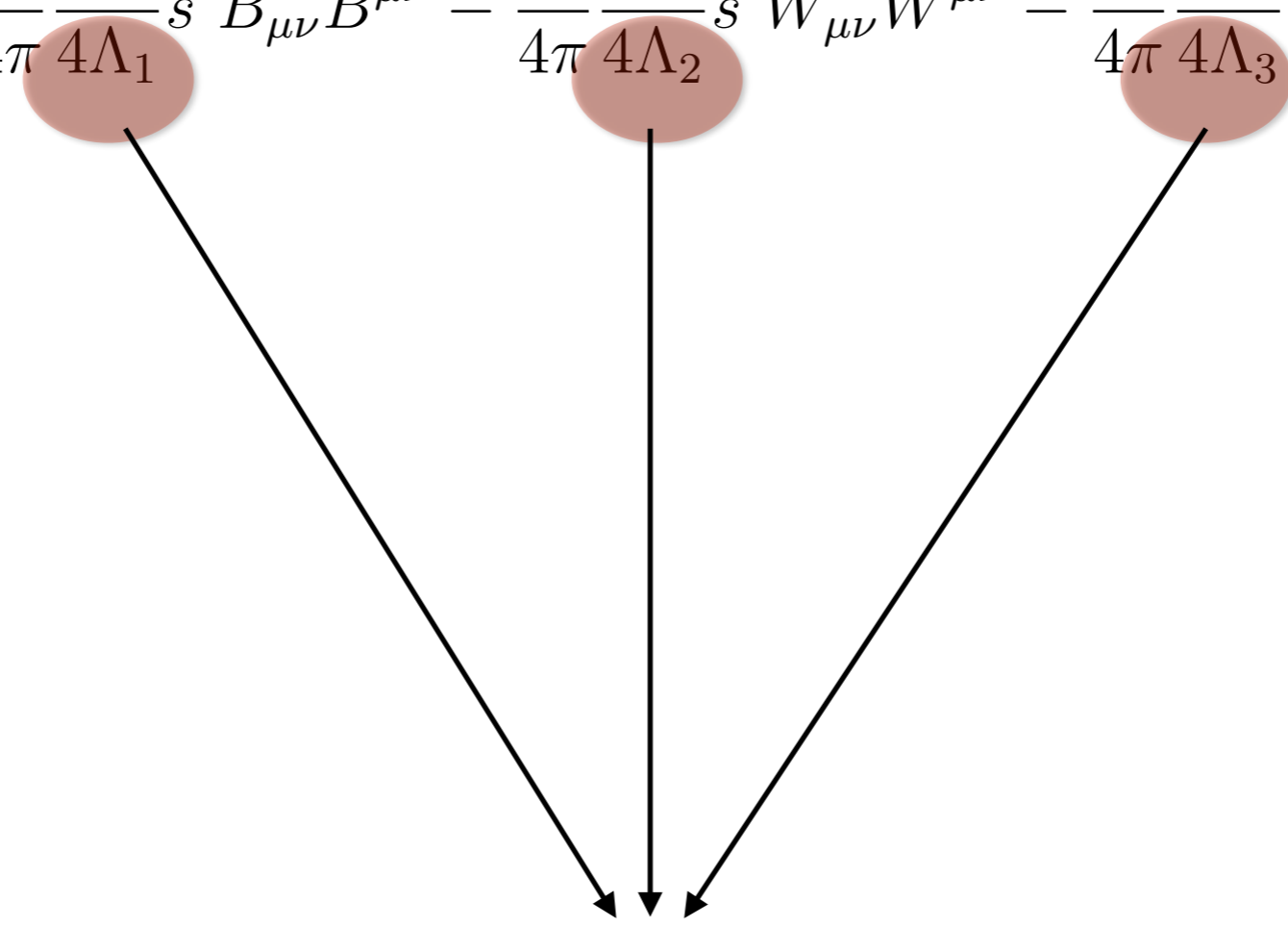
Effective couplings to gauge bosons

750 GeV portal to DM

- Coupling of a 750 scalar resonance to gauge bosons and dark matter particle
- $d = 5$ effective Lagrangian, Majorana fermion dark matter

$$\mathcal{L}_{\text{NP,CPE}} = \frac{1}{2}(\partial_\mu s)^2 - \frac{\mu_s^2}{2}s^2 + \frac{1}{2}\bar{\psi}(i\cancel{\partial}_\mu - m_\psi)\psi - \frac{y_\psi}{2}s\bar{\psi}\psi$$

$$- \frac{g_1^2}{4\pi} \frac{1}{4\Lambda_1} s B_{\mu\nu} B^{\mu\nu} - \frac{g_2^2}{4\pi} \frac{1}{4\Lambda_2} s W_{\mu\nu} W^{\mu\nu} - \frac{g_3^2}{4\pi} \frac{1}{4\Lambda_3} s G_{\mu\nu} G^{\mu\nu}$$



Mass scales for effective couplings

750 GeV portal to DM

- Coupling of a 750 scalar resonance to gauge bosons and dark matter particle
- $d = 5$ effective Lagrangian, Majorana fermion dark matter

$$\mathcal{L}_{\text{NP,CPE}} = \frac{1}{2}(\partial_\mu s)^2 - \frac{\mu_s^2}{2}s^2 + \frac{1}{2}\bar{\psi}(i\cancel{\partial}_\mu - m_\psi)\psi - \frac{y_\psi}{2}s\bar{\psi}\psi$$

$$- \frac{g_1^2}{4\pi} \frac{1}{4\Lambda_1} s B_{\mu\nu} B^{\mu\nu} - \frac{g_2^2}{4\pi} \frac{1}{4\Lambda_2} s W_{\mu\nu} W^{\mu\nu} - \frac{g_3^2}{4\pi} \frac{1}{4\Lambda_3} s G_{\mu\nu} G^{\mu\nu}$$

SM gauge couplings



750 GeV portal to DM

- Coupling of a 750 scalar resonance to gauge bosons and dark matter particle
- $d = 5$ effective Lagrangian, Majorana fermion dark matter

$$\mathcal{L}_{\text{NP,CPE}} = \frac{1}{2}(\partial_\mu s)^2 - \frac{\mu_s^2}{2}s^2 + \frac{1}{2}\bar{\psi}(i\cancel{\partial}_\mu - m_\psi)\psi - \frac{y_\psi}{2}s\bar{\psi}\psi$$

$$- \frac{g_1^2}{4\pi} \frac{1}{4\Lambda_1} s B_{\mu\nu} B^{\mu\nu} - \frac{g_2^2}{4\pi} \frac{1}{4\Lambda_2} s W_{\mu\nu} W^{\mu\nu} - \frac{g_3^2}{4\pi} \frac{1}{4\Lambda_3} s G_{\mu\nu} G^{\mu\nu}$$

Coupling to DM
(controls width of s)

750 GeV portal to DM

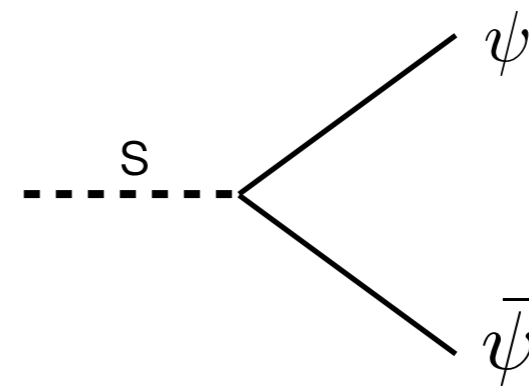
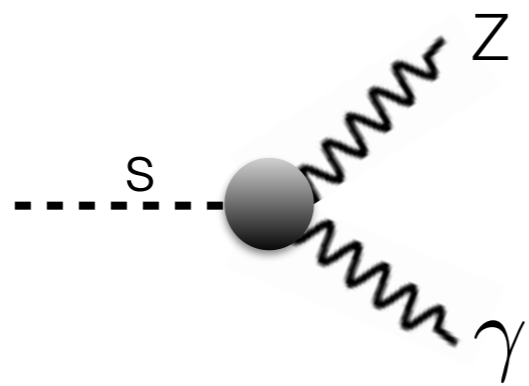
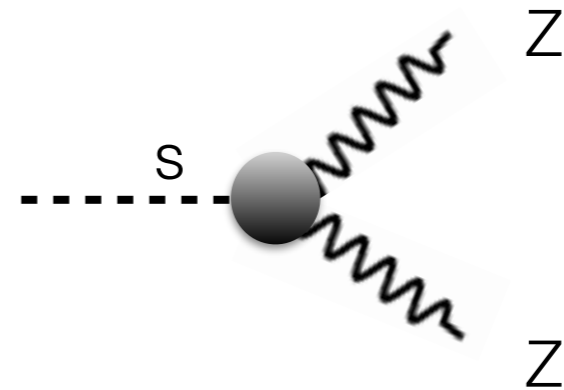
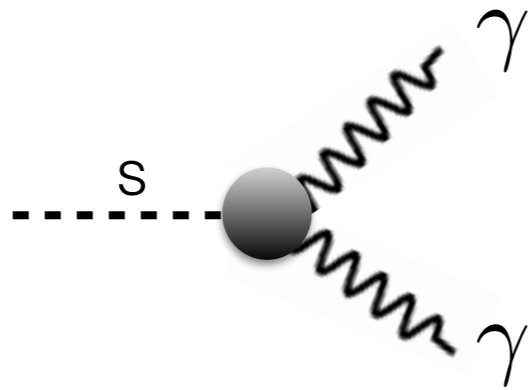
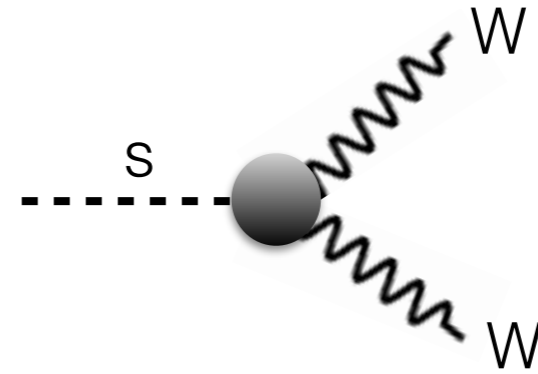
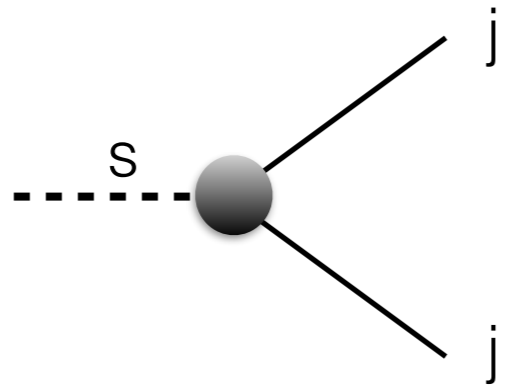
- Coupling of a 750 scalar resonance to gauge bosons and dark matter particle
- $d = 5$ effective Lagrangian, Majorana fermion dark matter

$$\mathcal{L}_{\text{NP,CPE}} = \frac{1}{2}(\partial_\mu s)^2 - \frac{\mu_s^2}{2}s^2 + \frac{1}{2}\bar{\psi}(i\cancel{\partial}_\mu - m_\psi)\psi - \frac{y_\psi}{2}s\bar{\psi}\psi$$

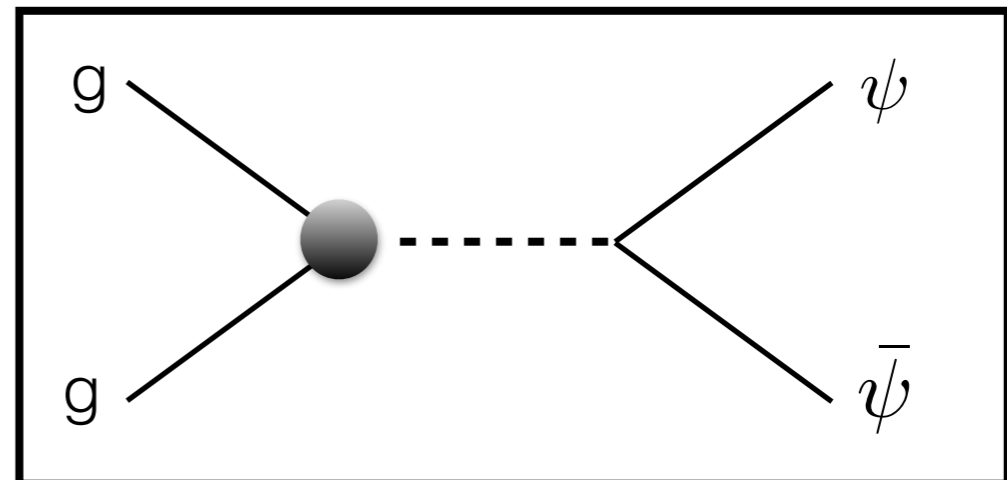
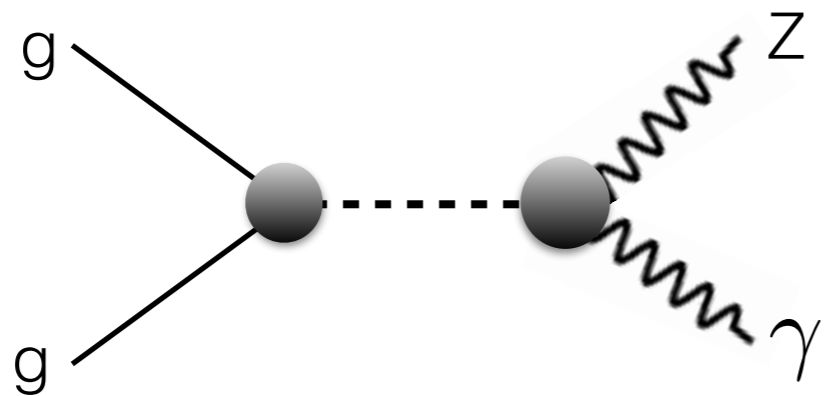
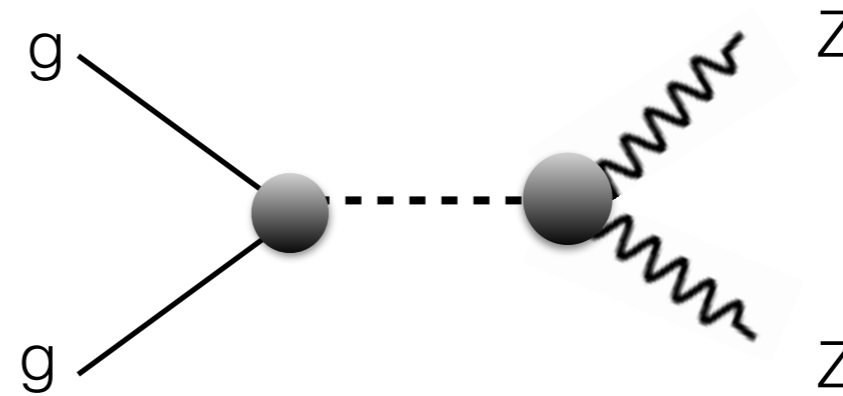
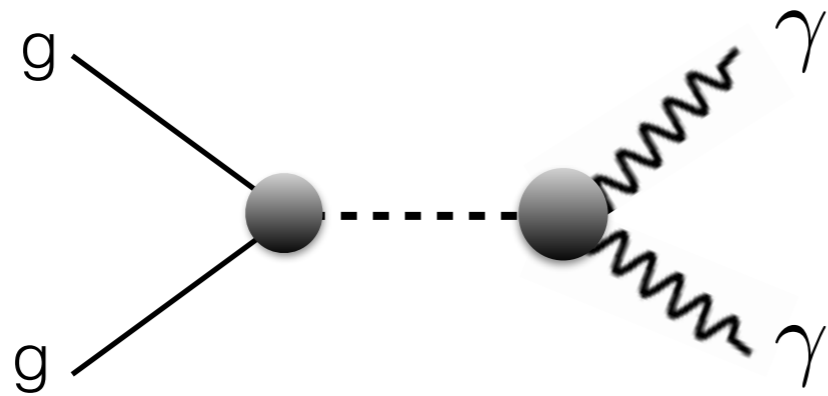
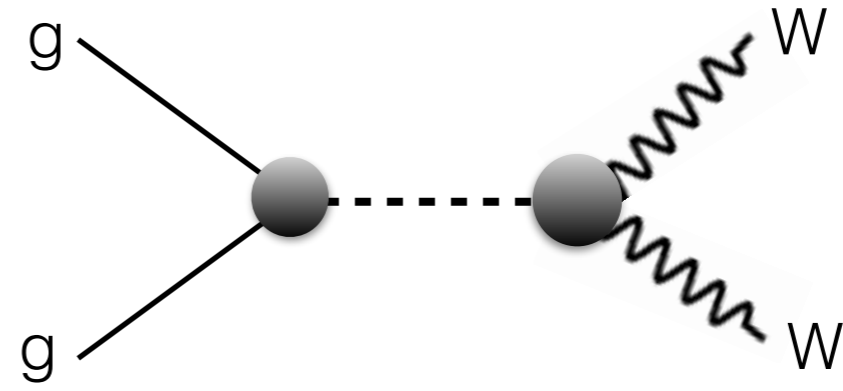
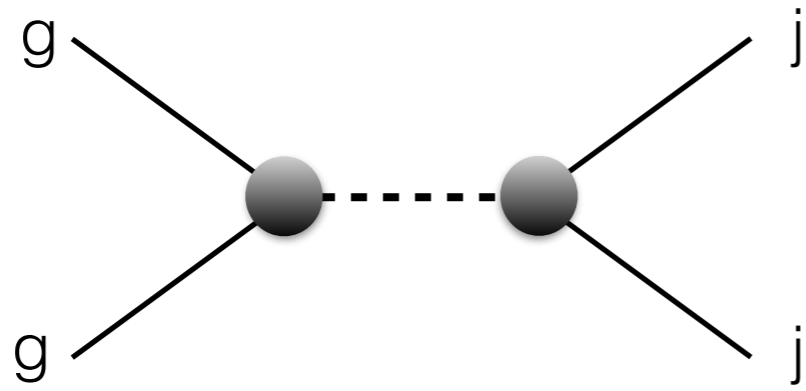
$$- \frac{g_1^2}{4\pi} \frac{1}{4\Lambda_1} s B_{\mu\nu} B^{\mu\nu} - \frac{g_2^2}{4\pi} \frac{1}{4\Lambda_2} s W_{\mu\nu} W^{\mu\nu} - \frac{g_3^2}{4\pi} \frac{1}{4\Lambda_3} s G_{\mu\nu} G^{\mu\nu}$$

Mass term 750 GeV

Decays

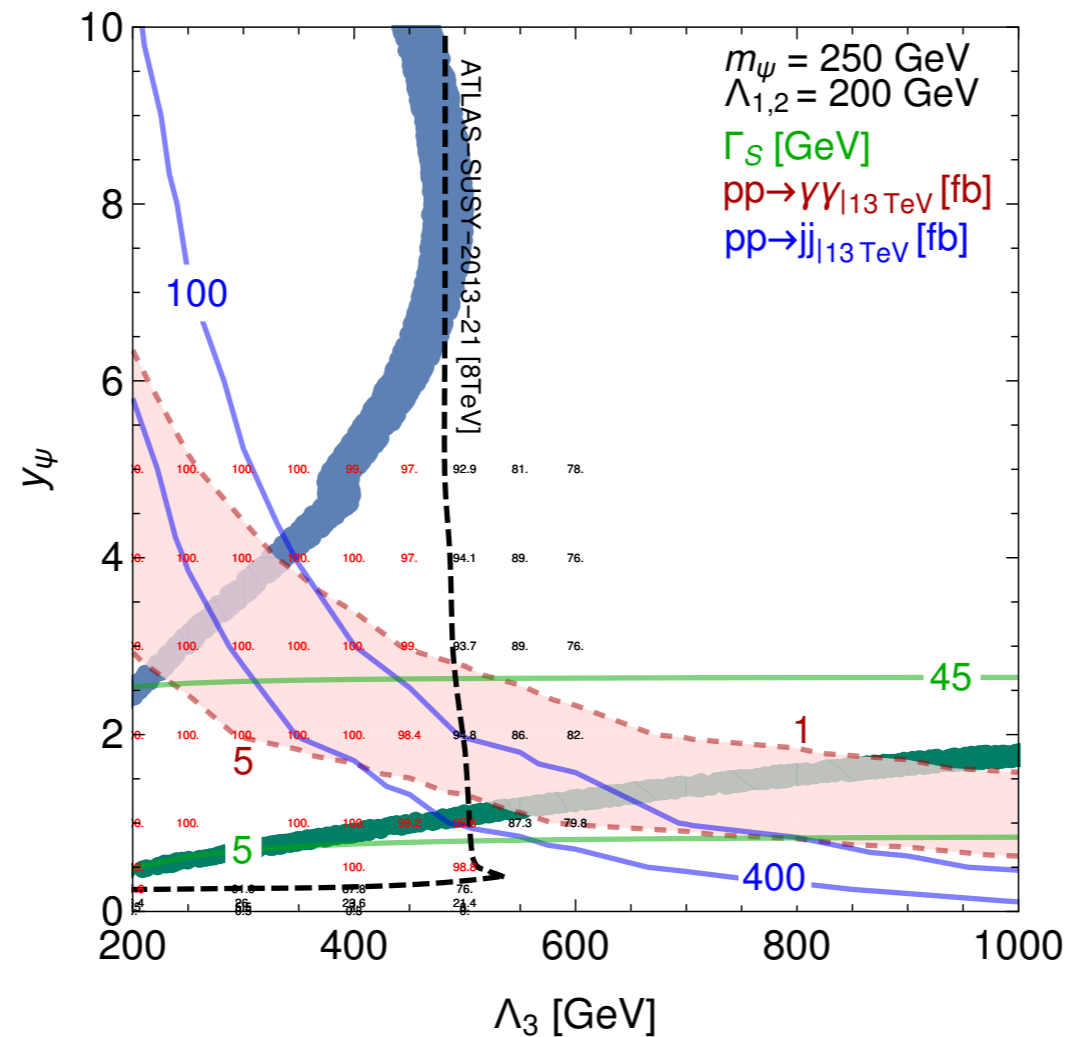


LHC phenomenology



Melange des constraints

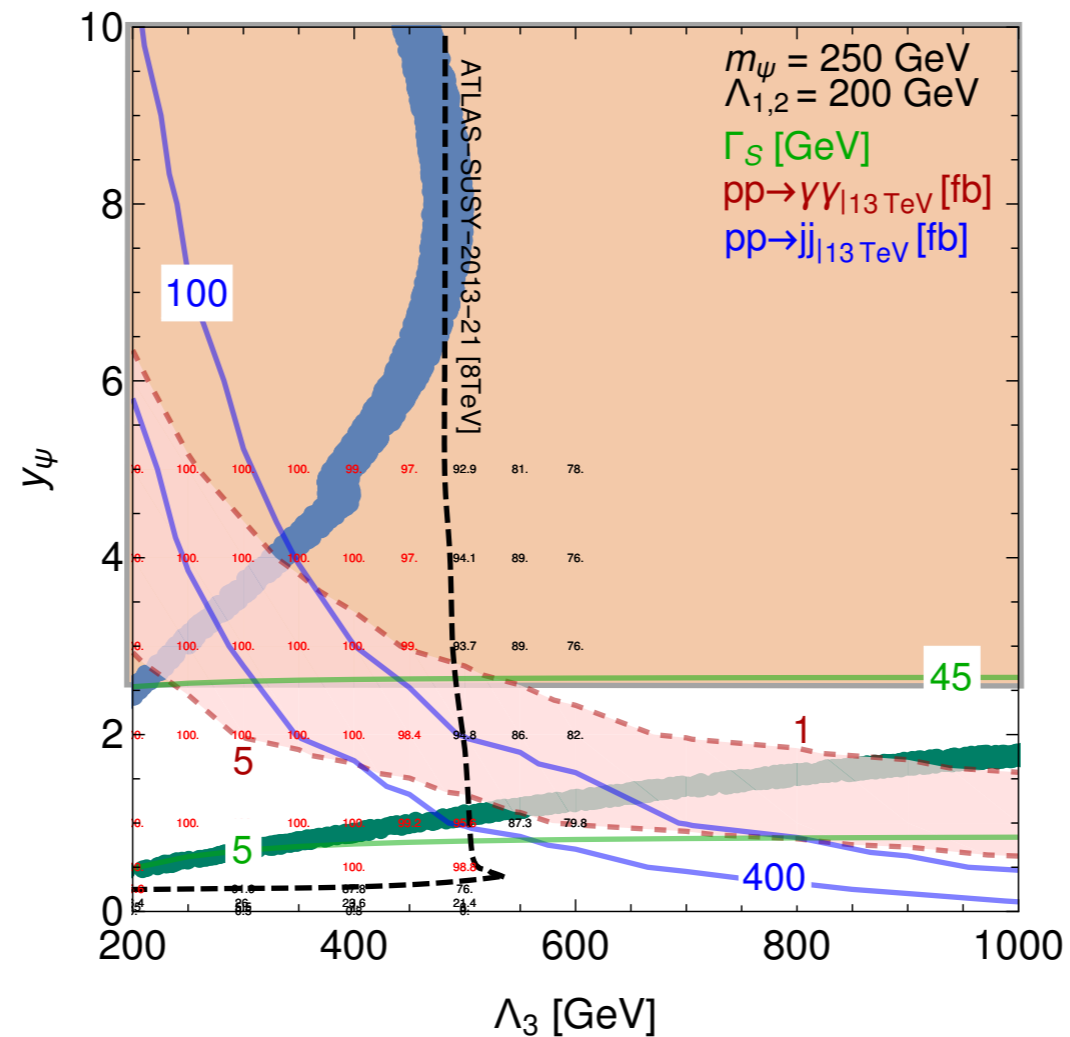
Barducci et al arXiv: 1512.06842



- Using ATLAS SUSY analysis it is possible to constrain the parameter space for diphoton excess models connected to dark matter

Melange des constraints

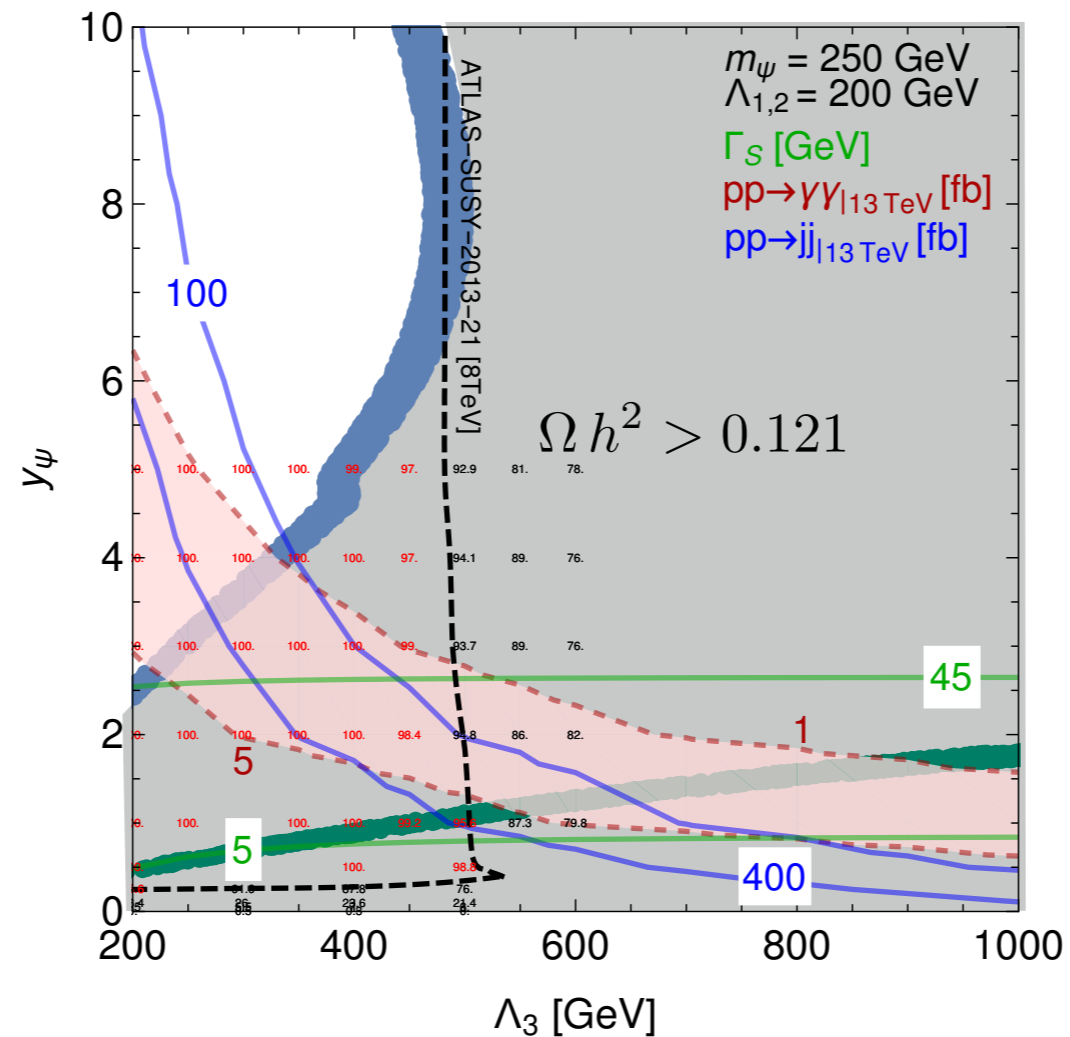
Barducci et al arXiv: 1512.06842



- Using ATLAS SUSY analysis it is possible to constrain the parameter space for diphoton excess models connected to dark matter

Melange des constraints

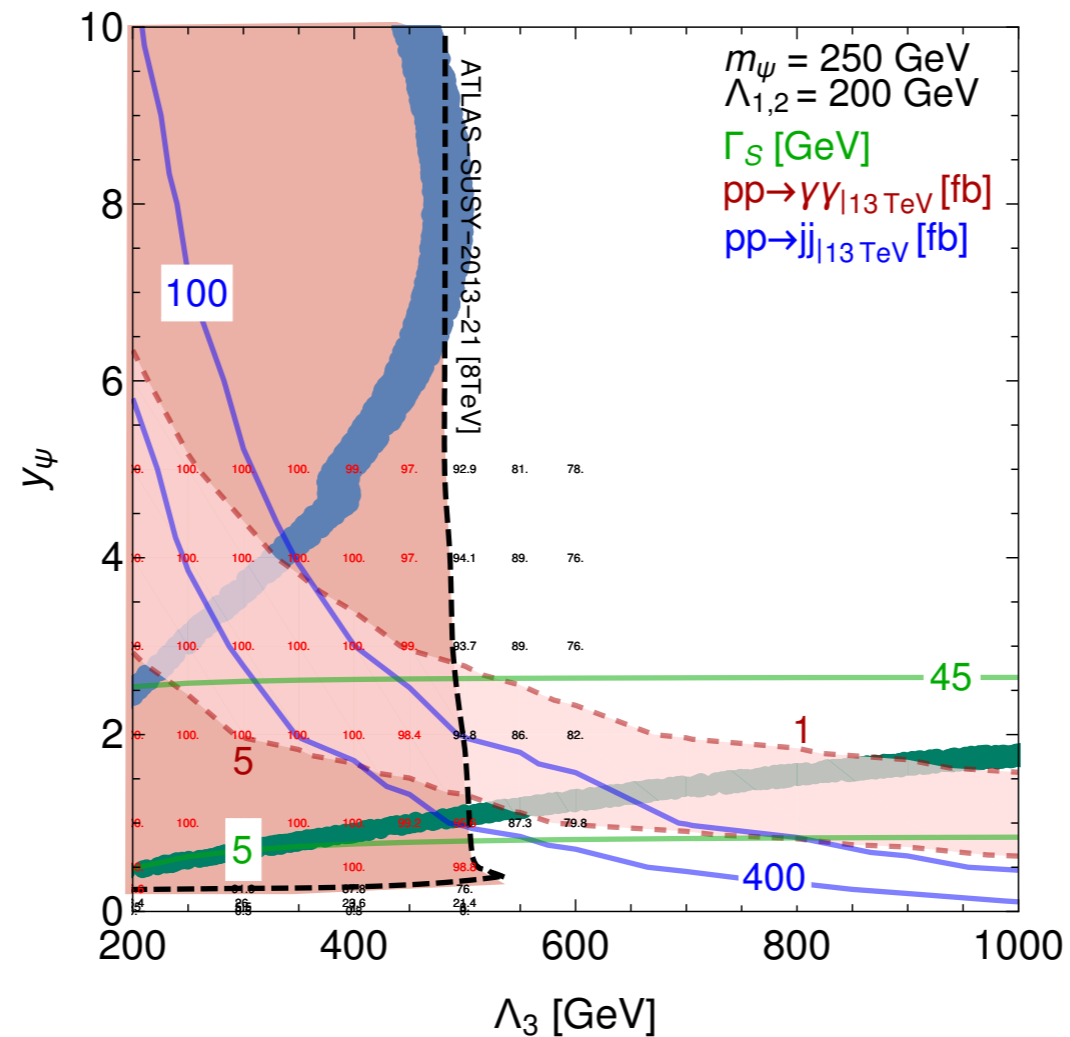
Barducci et al arXiv: 1512.06842



- Using ATLAS SUSY analysis it is possible to constrain the parameter space for diphoton excess models connected to dark matter

Melange des constraints

Barducci et al arXiv: 1512.06842



- Using ATLAS SUSY analysis it is possible to constrain the parameter space for diphoton excess models connected to dark matter

Test case: II

Exploring momentum dependent dark matter couplings

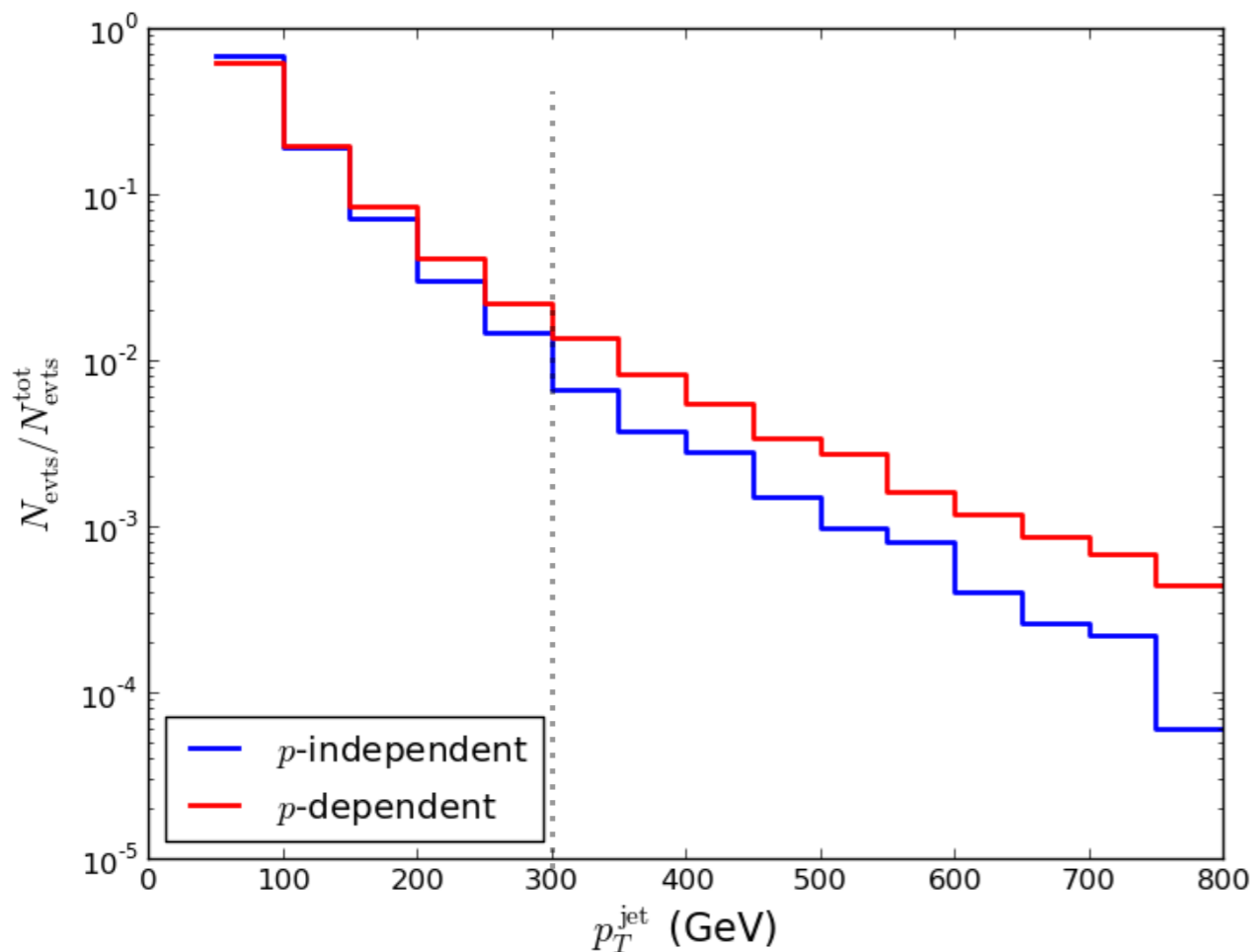
Impact on monojets

- Operators generally considered at the LHC

$$\mathcal{L}_{\text{vector}} = g_q \sum_{q=u,d,s,c,b,t} Z'_\mu \bar{q} \gamma^\mu q + g_\chi Z'_\mu \bar{\chi} \gamma^\mu \chi$$

$$\mathcal{L}_{\text{axial-vector}} = g_q \sum_{q=u,d,s,c,b,t} Z'_\mu \bar{q} \gamma^\mu \gamma^5 q + g_\chi Z'_\mu \bar{\chi} \gamma^\mu \gamma^5 \chi.$$

- What about more complicated interactions, e.g. momentum dependent ones?

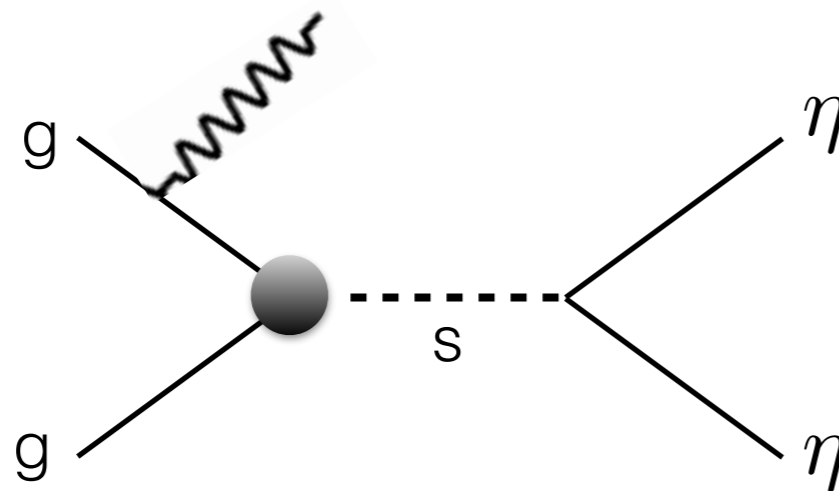


$$ig_{h\eta\eta} = 2iv \left[\lambda_{\text{mi}} + \frac{p_h^2}{f^2} \right]$$

- Z_2 odd real singlet scalar dark matter particle couplings to the Standard Model with Z_2 even scalar singlet

$$\mathcal{L}_{\eta,s} = \mathcal{L}_{\text{SM}} + \frac{1}{2} \partial_\mu \eta \partial^\mu \eta - \frac{1}{2} m_\eta^2 \eta \eta + \frac{1}{2} \partial_\mu s \partial^\mu s - \frac{1}{2} m_s^2 s s$$

$$+ \frac{c_{s\eta} f}{2} s \eta \eta + \frac{c_{\partial s \eta}}{f} (\partial_\mu s) (\partial^\mu \eta) \eta + \frac{\alpha_s}{16\pi} \frac{c_{sg}}{f} s G_{\mu\nu}^a G^{a\mu\nu}$$

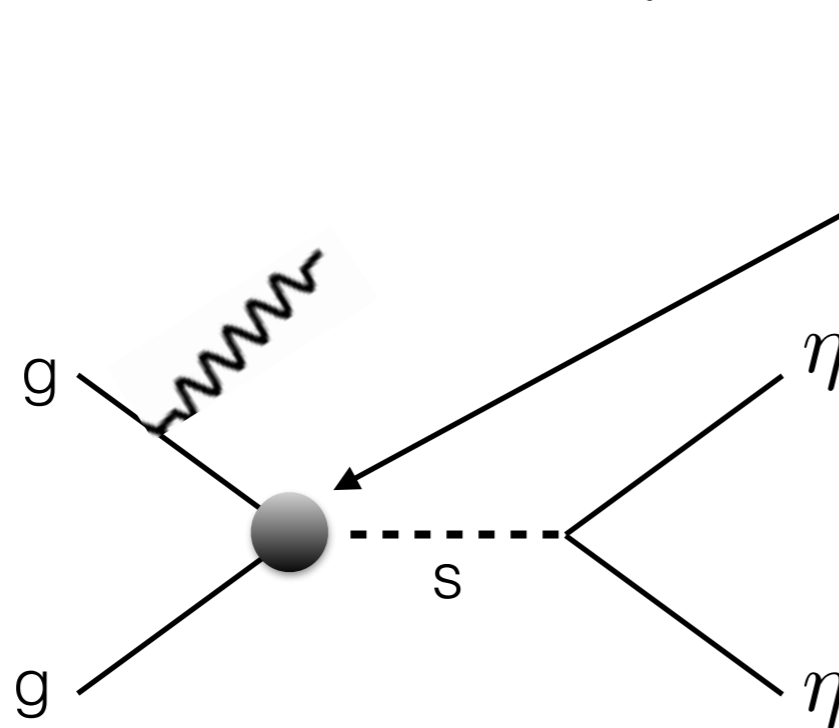


For consistent model constructions and detailed dark matter phenomenology see Fonseca et al. arXiv:1501.05957

- Z_2 odd real singlet scalar dark matter particle couplings to the Standard Model with Z_2 even scalar singlet

$$\mathcal{L}_{\eta,s} = \mathcal{L}_{\text{SM}} + \frac{1}{2} \partial_\mu \eta \partial^\mu \eta - \frac{1}{2} m_\eta^2 \eta \eta + \frac{1}{2} \partial_\mu s \partial^\mu s - \frac{1}{2} m_s^2 s s$$

$$+ \frac{c_{s\eta} f}{2} s \eta \eta + \frac{c_{\partial s \eta}}{f} (\partial_\mu s) (\partial^\mu \eta) \eta + \frac{\alpha_s}{16\pi} \frac{c_{sg}}{f} s G_{\mu\nu}^a G^{a\mu\nu}$$

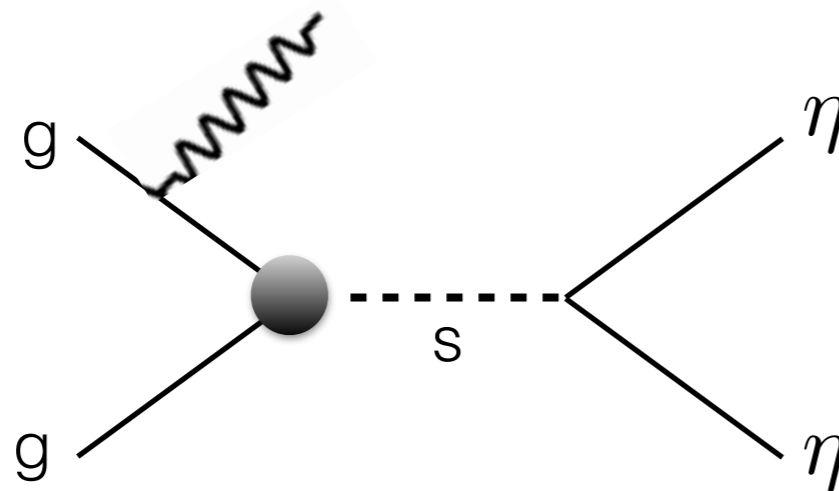


For consistent model constructions and detailed dark matter phenomenology see Fonseca et al. arXiv:1501.05957

- Z_2 odd real singlet scalar dark matter particle couplings to the Standard Model with Z_2 even scalar singlet

$$\mathcal{L}_{\eta,s} = \mathcal{L}_{\text{SM}} + \frac{1}{2} \partial_\mu \eta \partial^\mu \eta - \frac{1}{2} m_\eta^2 \eta \eta + \frac{1}{2} \partial_\mu s \partial^\mu s - \frac{1}{2} m_s^2 s s$$

$$+ \frac{c_{s\eta} f}{2} s \eta \eta + \frac{c_{\partial s \eta}}{f} (\partial_\mu s) (\partial^\mu \eta) \eta + \frac{\alpha_s}{16\pi} \frac{c_{sg}}{f} s G_{\mu\nu}^a G^{a\mu\nu}$$

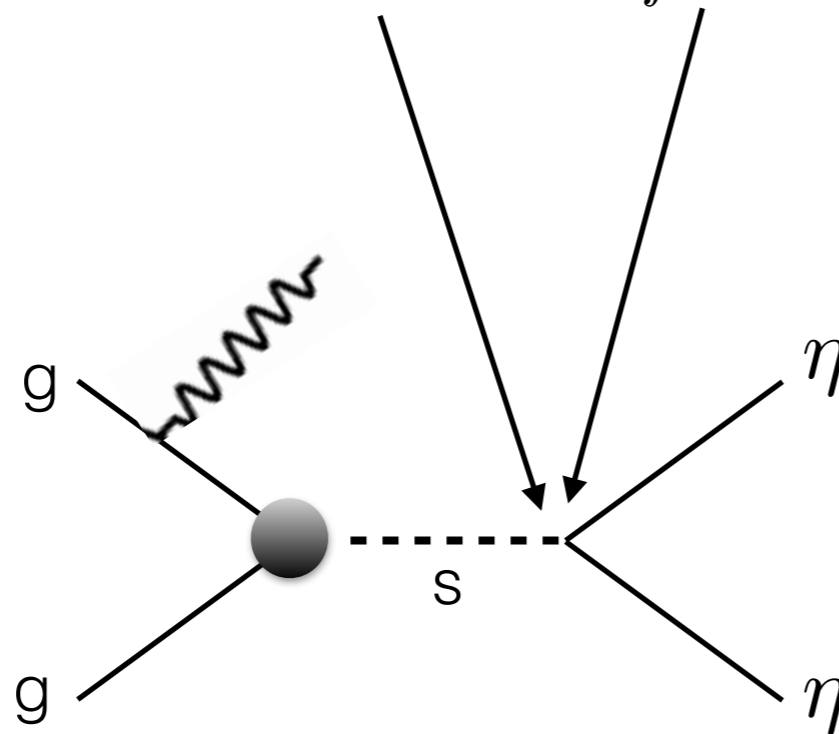


For consistent model constructions and detailed dark matter phenomenology see Fonseca et al. arXiv:1501.05957

- Z_2 odd real singlet scalar dark matter particle couplings to the Standard Model with Z_2 even scalar singlet

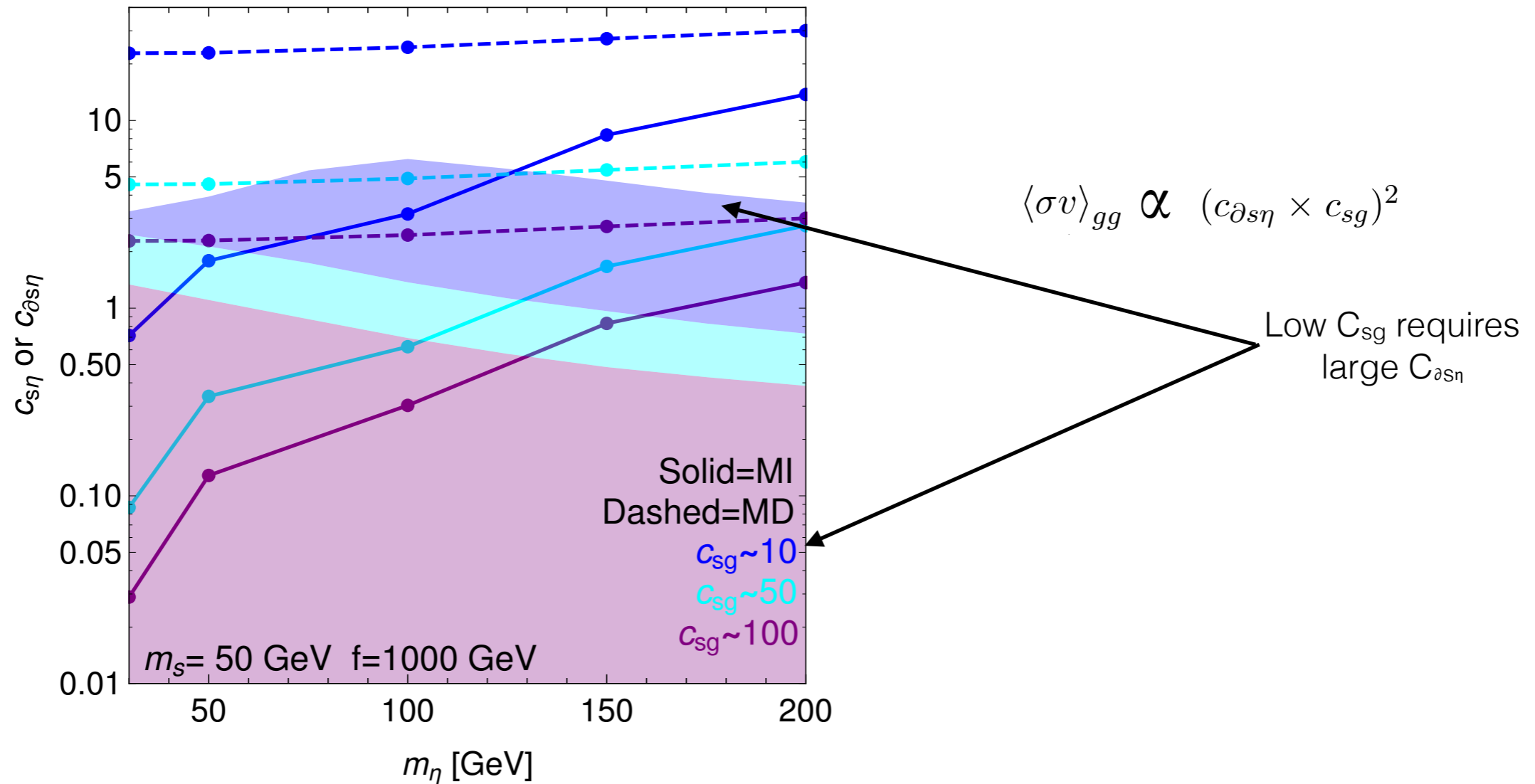
$$\mathcal{L}_{\eta,s} = \mathcal{L}_{\text{SM}} + \frac{1}{2} \partial_\mu \eta \partial^\mu \eta - \frac{1}{2} m_\eta^2 \eta \eta + \frac{1}{2} \partial_\mu s \partial^\mu s - \frac{1}{2} m_s^2 s s$$

$$+ \frac{c_{s\eta} f}{2} s \eta \eta + \frac{c_{\partial s \eta}}{f} (\partial_\mu s) (\partial^\mu \eta) \eta + \frac{\alpha_s}{16\pi} \frac{c_{sg}}{f} s G_{\mu\nu}^a G^{a\mu\nu}$$



For consistent model constructions and detailed dark matter phenomenology see Fonseca et al. arXiv:1501.05957

Limits



- Very different limits for momentum dependent and independent couplings
- LHC can not yet probe regions compatible relic density, situation might be more optimistic at 13 TeV searches (work in progress)

Conclusions

- Identifying the properties of dark matter is one of the challenges of 21st century
- Searches at the LHC can help constrain the properties of thermal dark matter
- The dark matter motivated explanations of 750 GeV diphoton excess are well constrained by the monojet searches
- Dark matter can also have momentum dependent couplings e.g. if dark matter is pNGB boson
 - The momentum dependent and independent couplings yield genuine differences in the p_T distributions of the jets and hence in the limits derived from monojet searches
 - Current limits from 8TeV monojet searches do not probe relic compatible region

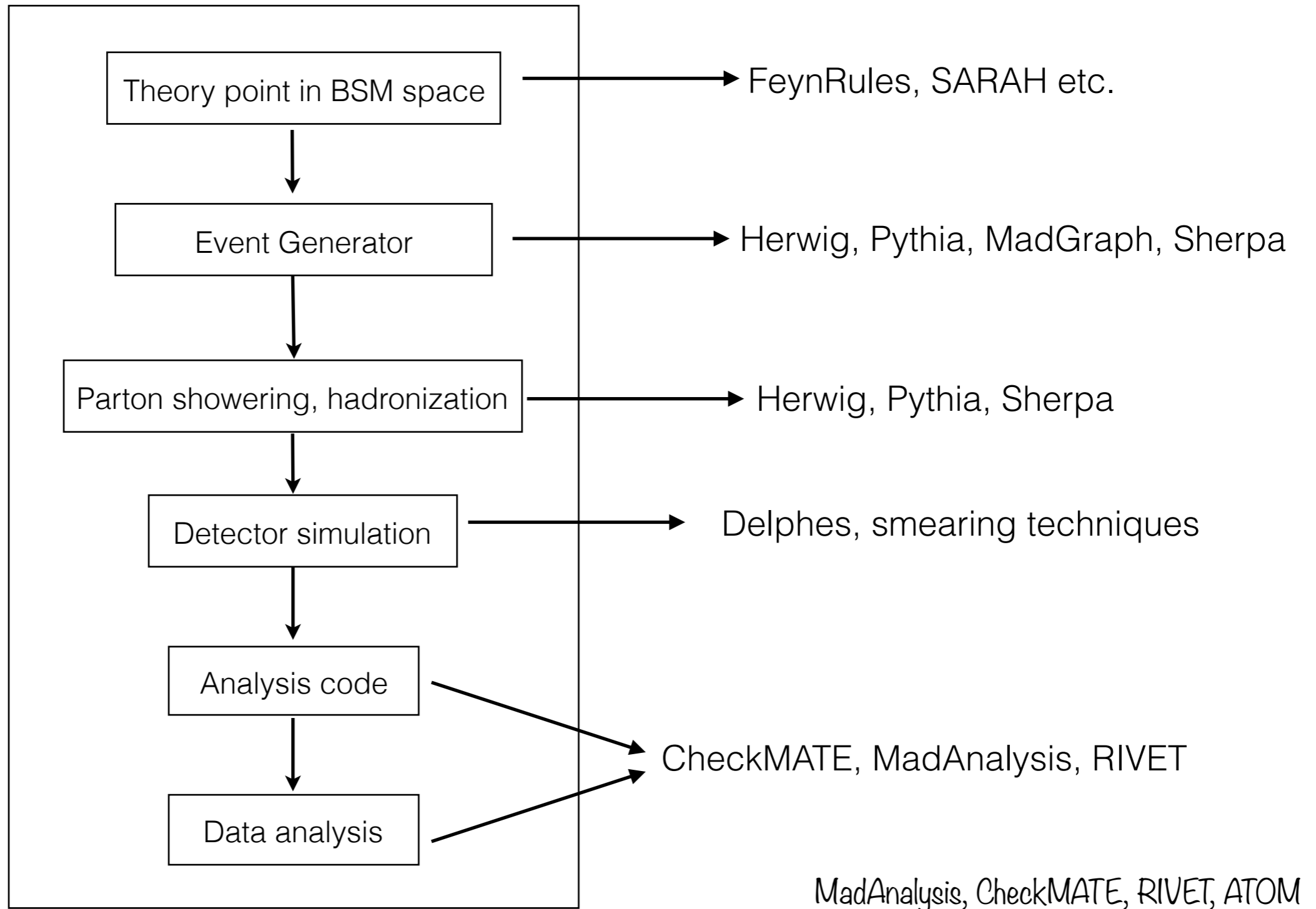


Backup

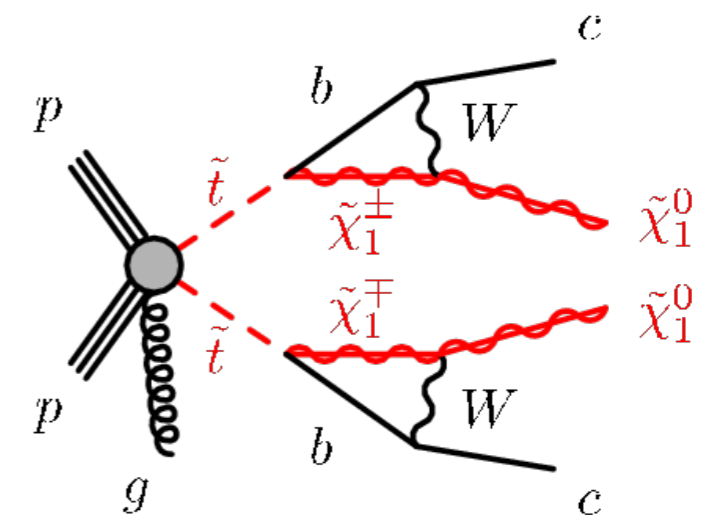
Test case: I

750 GeV as a portal to dark matter

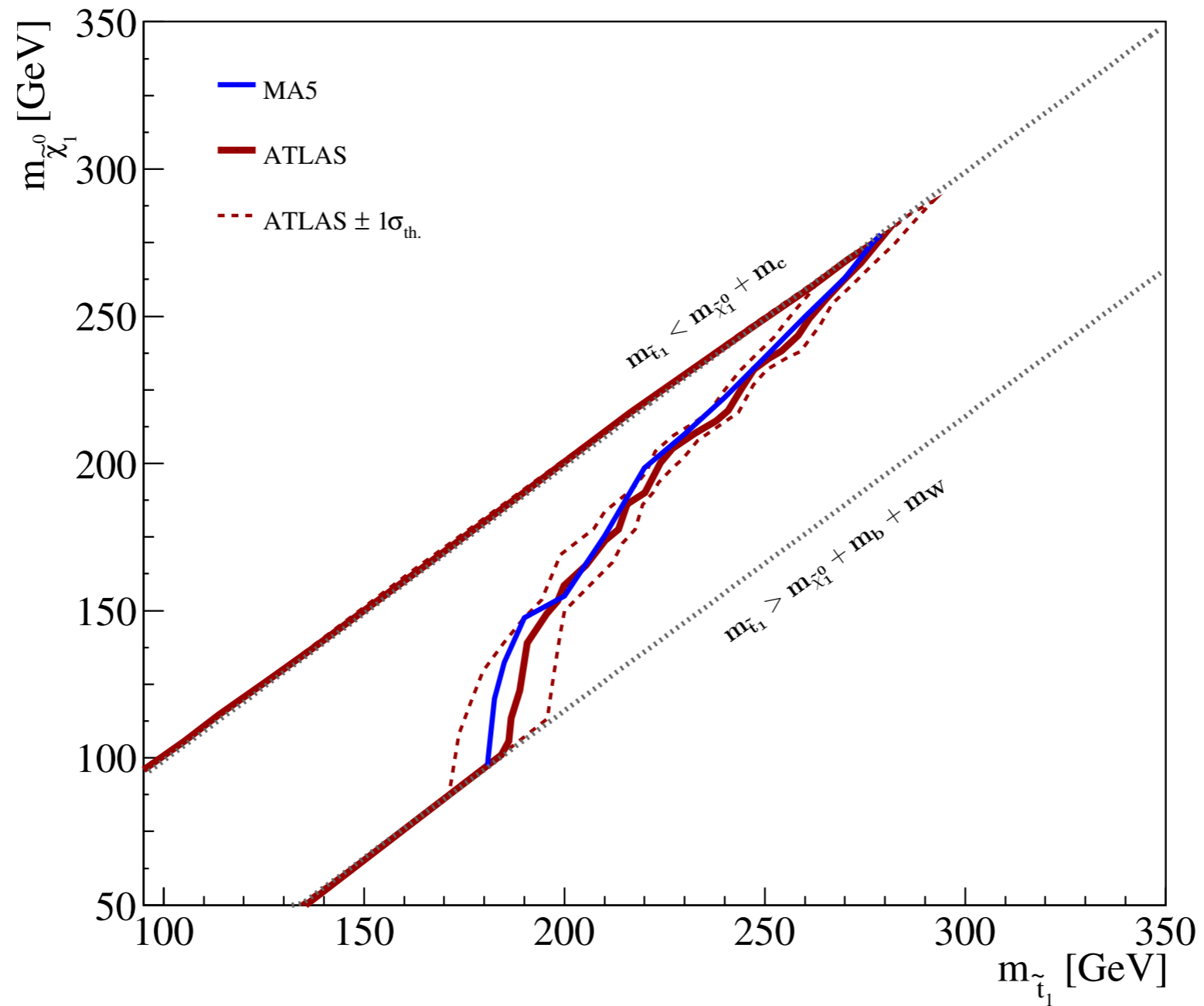
Analysis reinterpretation



- Search for compressed stops
- Considers monojet (ISR) and c-tagging
- Only monojet analysis implemented in MadAnalysis5



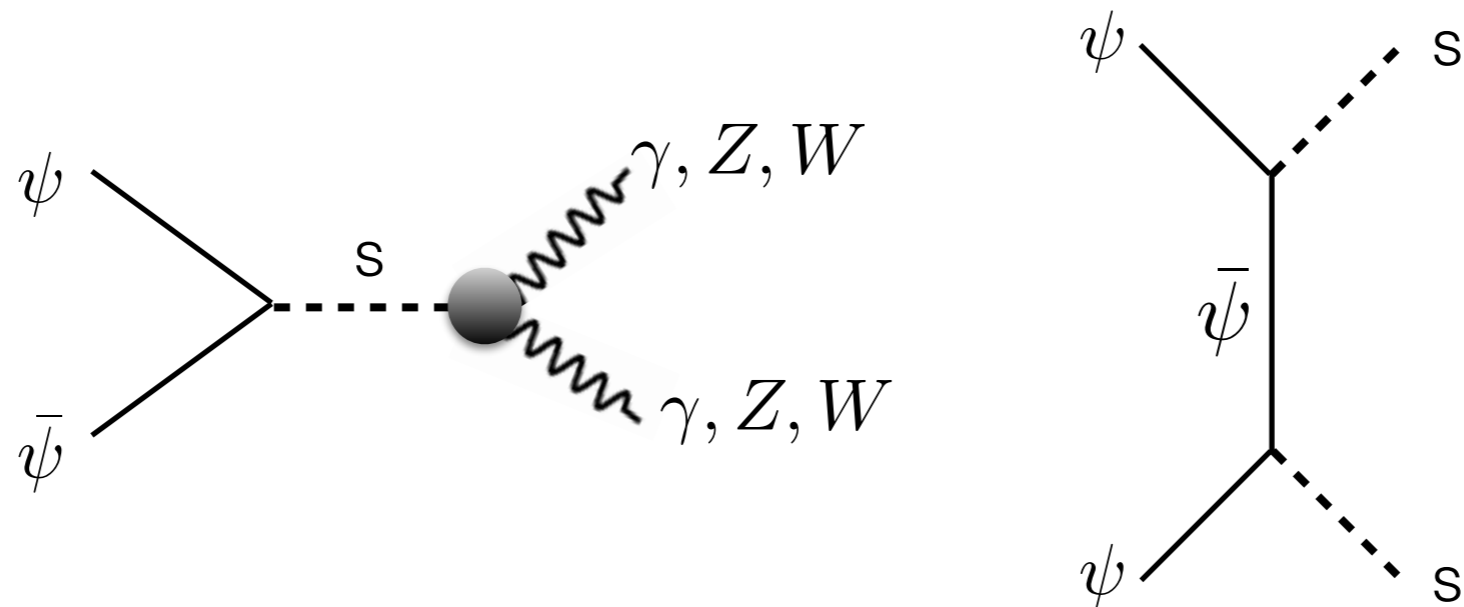
$\tilde{t} \rightarrow c\tilde{\chi}_1^0$ (200/125) cutflow				
cut	# events (scaled to σ and \mathcal{L})	relative change	# events (official)	relative change (official)
Initial number of events	376047.3	376047.3		
$E_T^{\text{miss}} > 80$ GeV Filter	192812.8	-48.7%	181902.0	181902.0
$E_T^{\text{miss}} > 100$ GeV	136257.1	-29.3%	97217.0	-46.6%
Trigger, Event cleaning...	-	-	82131.0	
Lepton veto	134894.2	-1.0%	81855.0	-15.8%
$N_{\text{jets}} \leq 3$	101653.7	-24.6%	59315.0	-27.5%
$\Delta\phi(E_T^{\text{miss}}, \text{jets}) > 0.4$	95568.8	-2.1%	54295.0	-8.5%
Leading jet $p_T > 150$ GeV	17282.8	-81.9%	14220.0	-73.8%
$E_T^{\text{miss}} > 150$ GeV	10987.8	-36.4%	9468.0	-33.4%
M1 Signal Region				
Leading jet $p_T > 280$ GeV	2031.2	-81.5%	1627.0	-82.8%
$E_T^{\text{miss}} > 220$ GeV	1517.6	-25.3%	1276.0	-21.6%
M2 Signal Region				
Leading jet $p_T > 340$ GeV	858.0	-92.2%	721.0	-92.4%
$E_T^{\text{miss}} > 340$ GeV	344.4	-59.9%	282.0	-60.9%
M3 Signal Region				
Leading jet $p_T > 450$ GeV	204.3	-98.1%	169.0	-98.2%
$E_T^{\text{miss}} > 450$ GeV	61.3	-70.0%	64.0	-62.1%



Dark matter relic

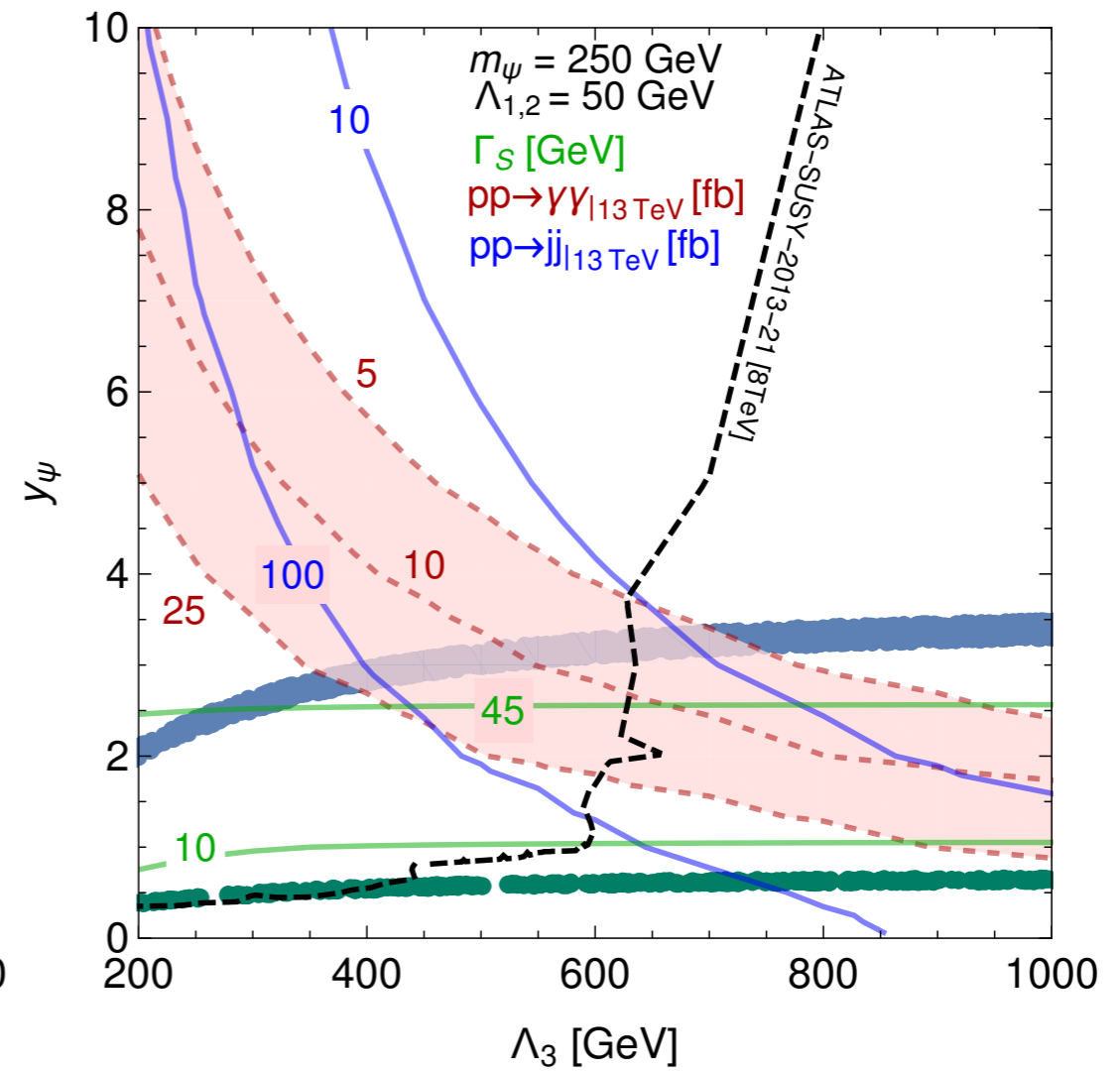
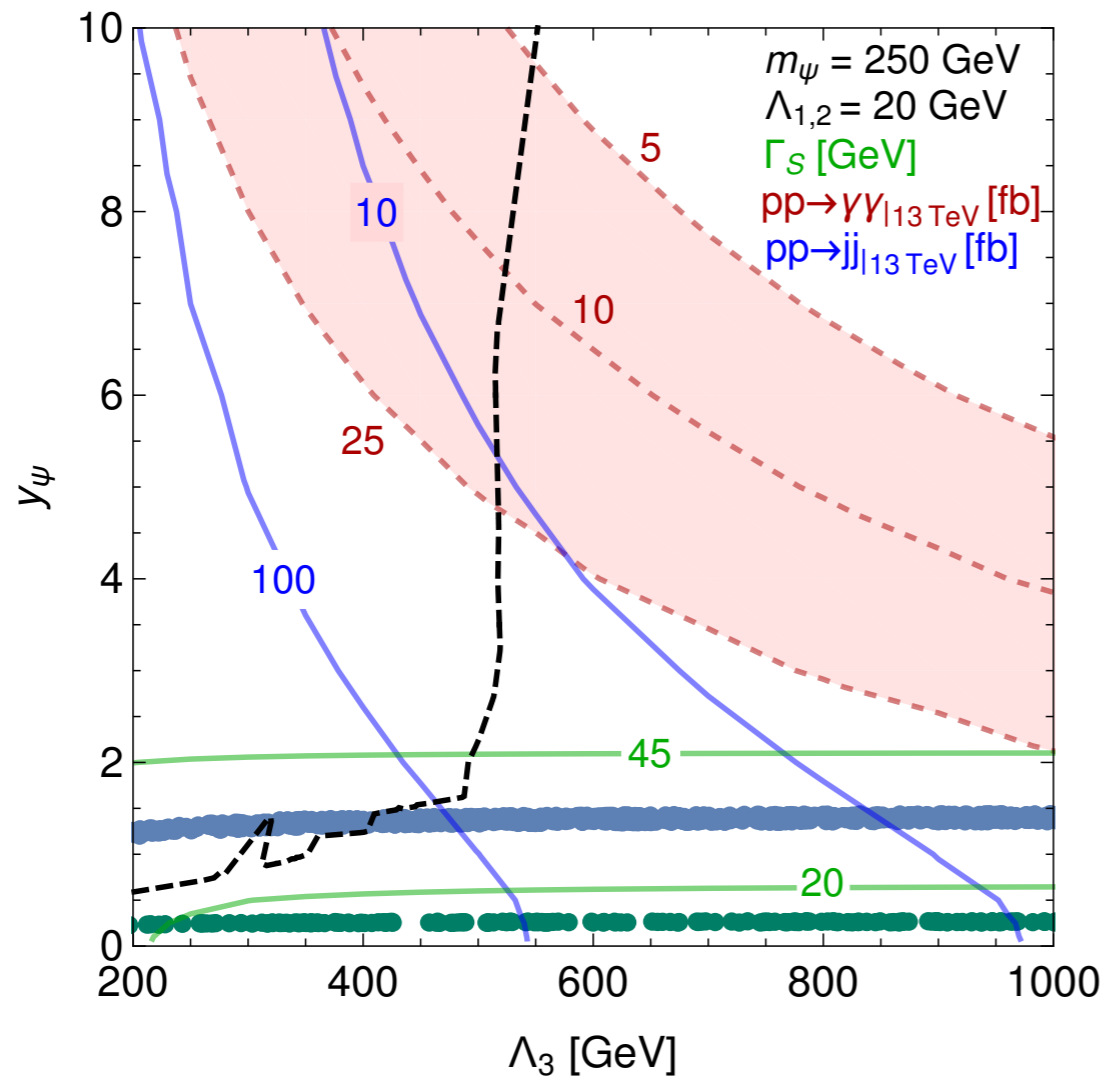
- CP even and CP odd couplings make a big difference for relic density
 - CP even case: p-wave suppression for annihilation cross section
 - Needs large values of Yukawa couplings to achieve relic
 - CP odd case: No velocity suppression much smaller values of Yukawa couplings work
-
- No couplings to fermions present
 - For dark matter mass less than 375 GeV, only gauge bosons, photons, and gg final states in s-channel present
 - For dark matter mass greater than 750 GeV t-channel annihilation into scalar resonance possible
 - Contribution up to 20% of the first scenario

Dark matter relic

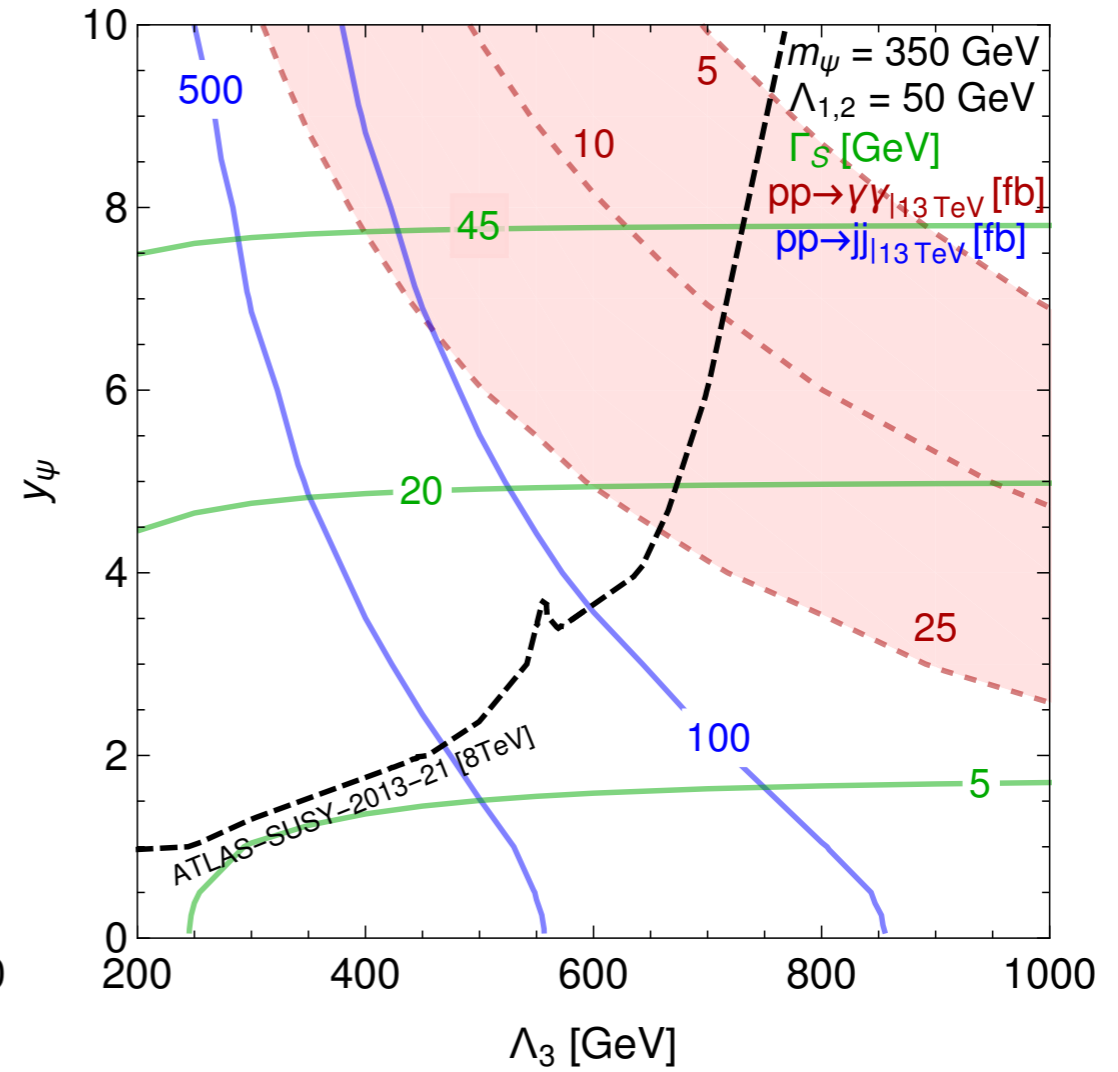
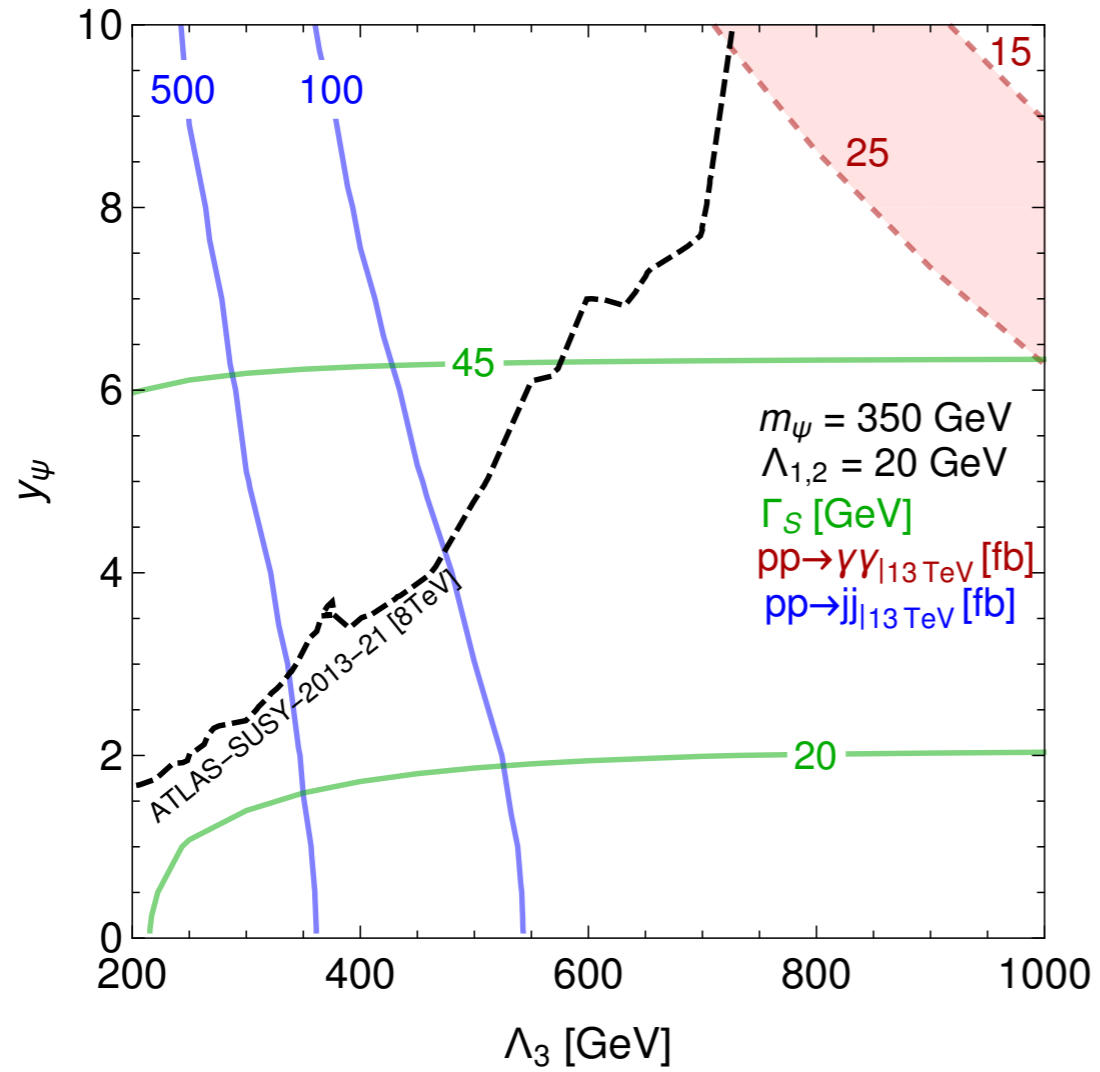


- No couplings to fermions present
- For dark matter mass less than 375 GeV, only gauge bosons, photons, and gg final states in s-channel present
- For dark matter mass greater than 750 GeV t-channel annihilation into scalar resonance possible
 - Contribution up to 20% of the first scenario

Additional results



Additional results



Test case: II

Exploring momentum dependent dark matter couplings

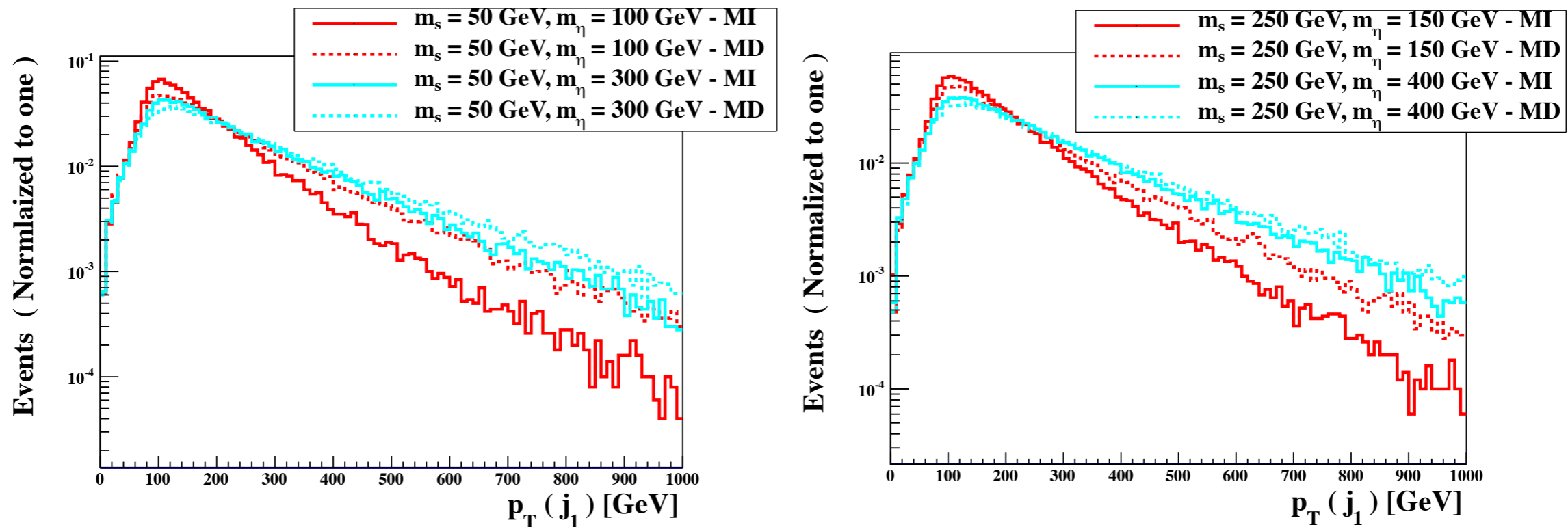
Propagator dependence

- The upper limits on the cross section are independent of the propagator mass

m_η	m_s	$\mathcal{A} \times \epsilon$ (SR1)		$\mathcal{A} \times \epsilon$ (SR2)		$\mathcal{A} \times \epsilon$ (SR3)		$\sigma_{UL}^{95\%CL}$ [pb]	
		MD	MI	MD	MI	MD	MI	MD	MI
200	50	0.123	0.101	0.073	0.056	0.033	0.023	0.317	0.465
200	250	0.124	0.104	0.069	0.054	0.031	0.022	0.349	0.487

Effect of momentum dependence

Barducci et al, to appear



$$c_{gs} = 100 \quad f = 1 \text{ TeV} \quad c_{\partial s\eta} = 2.5 \quad c_{s\eta} = 0.5$$

Production cross section of 2.9 pb after generator cut of jet $p_T > 80$ GeV

For $p_T > 300$ GeV,
Luminosity 300 fb^{-1}

#events MI	#events MD
131300	196533

Momentum dependent
expected to yield 50%
better sensitivity

Simple case

Barducci et al, arXiv:1605.02684

- Extension of the Standard Model by gauge singlet real scalar field

$$\mathcal{L}_\eta = \mathcal{L}_{SM} + \frac{1}{2}\partial_\mu\eta\partial^\mu\eta - \frac{1}{2}\mu_\eta^2\eta^2 - \frac{1}{4}\lambda_\eta\eta^4 - \frac{1}{2}\lambda\eta^2 H^\dagger H + \frac{1}{2f^2}(\partial_\mu\eta^2)\partial^\mu(H^\dagger H)$$

- After electroweak symmetry breaking

$$\mathcal{L}_\eta \supset -\frac{1}{4}(v+h)^2 \left(\lambda\eta^2 + \frac{1}{f^2}\partial_\mu\partial^\mu\eta^2 \right) \quad m_\eta^2 = \mu_\eta^2 + \lambda v^2/2$$

scale of spontaneous
symmetry breaking

Momentum dependent coupling

For mono-Higgs signature study of similar model
see e.g. arXiv:1312.2592

Simple case

- Extension of the Standard Model by gauge singlet real scalar field

$$\mathcal{L}_\eta = \mathcal{L}_{SM} + \frac{1}{2} \partial_\mu \eta \partial^\mu \eta - \frac{1}{2} \mu_\eta^2 \eta^2 - \frac{1}{4} \lambda_\eta \eta^4 - \frac{1}{2} \lambda \eta^2 H^\dagger H + \frac{1}{2f^2} (\partial_\mu \eta^2) \partial^\mu (H^\dagger H)$$

- Monojet production cross section

$$\hat{\sigma}(gg \rightarrow gh^* \rightarrow g\eta\eta) \propto \frac{\theta(p_h^2 - 4m_\eta^2)}{(p_h^2 - m_h^2)^2 + \Gamma_h^2 m_h^2} \left(\frac{p_h^2}{f^2} - \lambda \right)^2 \sqrt{1 - \frac{4m_\eta^2}{p_h^2}}$$

cross section < 1 fb

cross section < 0.5 fb

momentum dependent

momentum independent

On-shell production $p_h^2 = m_h^2$

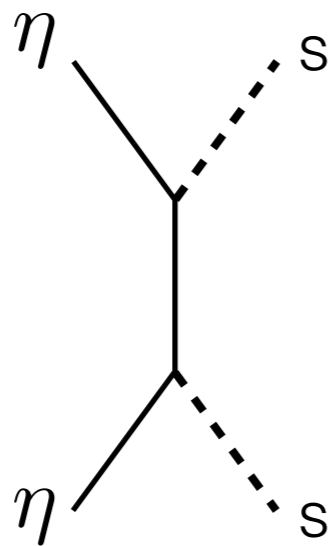
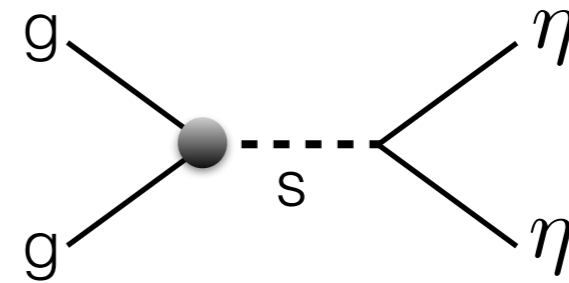
No momentum dependence

- Good measurements of Higgs production cross sections limit ggh couplings, decreasing the total cross section for monojet production

Relic density

- Unlike LHC constraints, relic density depends on the propagator mass
- Two annihilation channels

$$\langle \sigma v \rangle_{gg} \simeq \frac{\alpha_s^2 c_{sg}^2 (c_{s\eta} f^2 + 4c_{\partial s\eta} m_s^2)^2}{256\pi^3 f^4 (m_s^2 - 4m_\eta^2)^2}$$



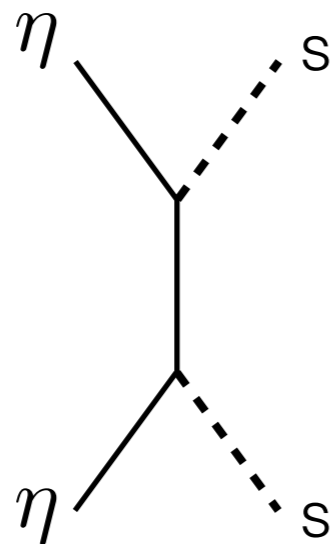
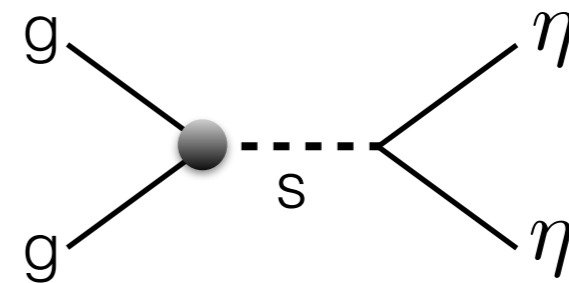
$$\langle \sigma v \rangle_{ss} \simeq \frac{\sqrt{1 - \frac{m_s^2}{m_\eta^2}} (c_{\partial s\eta} m_s^2 + c_{s\eta} f^2)^4}{16\pi f^4 m_\eta^2 (m_s^2 - 2m_\eta^2)^2}$$

Relic density

- Unlike LHC constraints, relic density depends on the propagator mass
- Two annihilation channels

Mostly drives relic

$$\langle \sigma v \rangle_{gg} \simeq \frac{\alpha_s^2 c_{sg}^2 (c_{s\eta} f^2 + 4c_{\partial s\eta} m_s^2)^2}{256\pi^3 f^4 (m_s^2 - 4m_\eta^2)^2}$$



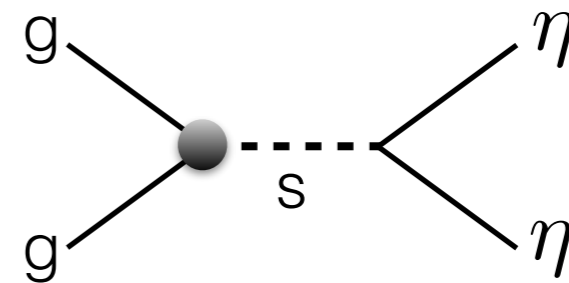
$$\langle \sigma v \rangle_{ss} \simeq \frac{\sqrt{1 - \frac{m_s^2}{m_\eta^2}} (c_{\partial s\eta} m_s^2 + c_{s\eta} f^2)^4}{16\pi f^4 m_\eta^2 (m_s^2 - 2m_\eta^2)^2}$$

Relic density

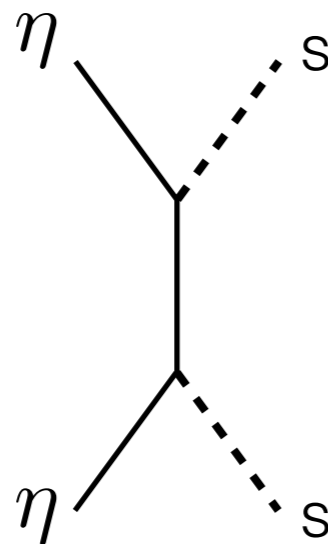
- Unlike LHC constraints, relic density depends on the propagator mass
- Two annihilation channels

Mostly drives relic

$$\langle \sigma v \rangle_{gg} \simeq \frac{\alpha_s^2 c_{sg}^2 (c_{s\eta} f^2 + 4c_{\partial s\eta} m_s^2)^2}{256\pi^3 f^4 (m_s^2 - 4m_\eta^2)^2}$$



Contributes up to 15%



$$\langle \sigma v \rangle_{ss} \simeq \frac{\sqrt{1 - \frac{m_s^2}{m_\eta^2}} (c_{\partial s\eta} m_s^2 + c_{s\eta} f^2)^4}{16\pi f^4 m_\eta^2 (m_s^2 - 2m_\eta^2)^2}$$